The Cosmic Ray Distribution in Sagittarius B

Roland M. Crocker[1], David Jones[1,2], Raymond J. Protheroe[1], Jürgen Ott[2,6], Ron Ekers[2,7], Fulvio Melia[3,8], Todor Stanev[4], and Anne Green[5]

[1] *School of Physics and Chemistry*
University of Adelaide
5005, Australia
roland.crocker@adelaide.edu.au
djones,rprother@physics.adelaide.edu.au

[2] *Australia Telescope National Facility*
Marsfield,
2122, Australia
Juergen.Ott,Ron.Ekers@csiro.au

[3]*Physics Department and Steward Observatory,*
The University of Arizona, Tucson, AZ 85721
melia@physics.arizona.edu

[4]*Bartol Research Institute,*
The University of Delaware, Newark, DE 19716-2593
stanev@bartol.udel.edu

[5]*School of Physics,*
University of Sydney,
2006, Australia
agreen@physics.usyd.edu.au

[6]*Bolton Fellow*

[7]*Federation Fellow*

[8]*Sir Thomas Lyle Fellow and Miegunyah Fellow*

February 5, 2008

ABSTRACT

The HESS instrument has observed a diffuse flux of $\sim$ TeV γ-rays from a large solid angle around the Galactic center (GC). This emission is correlated with the distribution of gas in the region suggesting that the γ-rays originate in

collisions between cosmic ray hadrons (CRHs) and ambient matter. Of particular interest, HESS has detected γ-rays from the Sagittarius (Sgr) B Molecular Cloud Complex. Prompted by the suggestion of a hadronic origin for the gamma rays, we have examined archival 330 and 74 MHz Very Large Array radio data and 843 MHz Sydney University Molonglo Sky Survey data covering Sgr B, looking for synchrotron emission from secondary electrons and positrons (expected to be created in the same interactions that supply the observed gamma rays). Intriguingly, we have uncovered non-thermal emission, but at a level exceeding expectation. Adding to the overall picture, recent observations by the Atacama Pathfinder Experiment telescope show that the cosmic ray ionization rate is ten times greater in the Sgr B2 region of Sgr B than the local value. Lastly, Sgr B2 is also a very bright X-ray source. We examine scenarios for the spectra of CRHs and/or primary electrons that would reconcile all these different data. We determine that (i) a hard ($\sim E^{-2.2}$), high-energy ($\gtrsim$ TeV) population CRHs is unavoidably required by the HESS γ-ray data and (ii) the remaining broad-band, non-thermal phenomenology is explained either by a rather steep ($\sim E^{-2.9}$) spectrum of primary electrons or a ($\sim E^{-2.7}$) population of CRHs. Perhaps unsurprisingly, no single, power-law population of either leptons or hadrons can explain the totality of broadband, non-thermal Sgr B phenomenology.

Subject headings: acceleration of particles—Galaxy: center—ISM: supernova remnants—radiation mechanisms: nonthermal

1. Introduction

The HESS air Cerenkov telescope located in Namibia has recently made a groundbreaking detection (Aharonian et al. 2006) of a diffuse flux (over a solid angle of approximately $4^\circ \times 2^\circ$) of γ-rays in the 0.2-20 TeV (1 TeV = 10^{12} eV) range emanating from the region of the Galactic center (GC) and distributed along the Galactic plane. This flux has been shown by the HESS collaboration to be correlated with the density of molecular gas (mostly H_2) pervading the region, as determined from CS measurements (Tsuboi et al. 1999), and argued, therefore, to originate primarily from neutral pion (and other meson) decay. These putative mesons would themselves be generated in collisions between cosmic

[1]Currently: Jansky Fellow, National Radio Astronomy Observatory 520 Edgemont Road, Charlottesville, VA 22903, email: jott@nrao.edu

ray protons or heavier ions (generically, cosmic ray hadrons; CRHs) and the ambient gas, the latter of which is contained in a number of giant molecular clouds complexes (GMCs), including the Sagittarius (Sgr) B complex. We label this broad idea 'the hadronic scenario'. Highly significantly for our purposes, the HESS collaboration has separately measured the γ-ray flux emanating from a $0.^\circ5 \times 0.^\circ5$ field centred on and covering the Sgr B GMC itself (defined in Galactic co-ordinates by $0.^\circ3 < l < 0.^\circ8$ and $-0.^\circ3 < b < 0.^\circ2$) and the spectrum of this emission.

Within the hadronic scenario, the well-known particle physics of pion (and heavier meson) production and subsequent decay together with the HESS γ-ray measurements allow us to make a prediction for the rate at which secondary electrons and positrons (generically, secondary leptons) would be injected into the Sgr B cloud through the same CR collision mechanism that, by hypothesis, supplies the γ-rays (CRH collisions lead to production of charged and neutral pions – and charged and neutral kaons – in roughly equal numbers and the charged pion and kaon decay chains ultimately terminate in the $e^\pm$ alluded to, together with neutrinos). With the additional input of the local magnetic field strength, the gas density, and the CRH spectral shape (viz., that the latter is a power-law in momentum as generically predicted by shock acceleration theory with a spectral index and normalization that match it smoothly on to the HESS observations) we can predict the synchrotron radio spectrum from $e^\pm$ secondaries generated over the entire Sgr B GMC. In fact, we can, on the basis of these inputs, self-consistently calculate the entire broadband spectrum of the Sgr B complex from radio to TeV energies, accounting for all relevant radiative processes (secondary electron synchrotron, bremsstrahlung and inverse Compton radiation as well as neutral meson decay).

The hadronic interpretation of the HESS data has recently been challenged by Yusef-Zadeh et al. (2006) who, remarking on an independent correlation between Fe Kα X-ray line emission and TeV γ-ray emission across the GC region, have suggested a model where a population (or populations) of *primary* electrons is responsible for the non-thermal emission seen from a number of molecular clouds, including Sgr B2. These authors suggest, in particular, that the TeV emission originate in inverse Compton (IC) scattering of sub-millimeter radiation from dust by the high energy component of the putative electron population. We label the broad idea that primary electrons are responsible for the bulk of the Sgr B phenomenology 'the leptonic scenario'.

We will examine the compatibility of both the hadronic and leptonic scenarios with the broadband non-thermal spectrum of Sgr B and other Sgr B phenomenology in detail in the current work.

2. Inferred Environment and Morphology of Sgr B

On the basis of CS measurements (Tsuboi et al. 1999), the HESS collaboration report that the mass of molecular material within the half degree by half degree field covering the Sgr B Complex is between 6 and 15 million solar masses. In the following we consider both these bounding values in modeling emission at various wavelengths from the region.

Sgr B is one of a number of GMCs bound in relatively tight orbits (projected distance of ~ 100 pc) around Sgr A*, the radio source associated with the supermassive ($\sim 3.7\times10^6\ M_\odot$) black hole at the center of the Galaxy (at an assumed distance of 8.5 kpc). Together these complexes constitute the central molecular zone, a structure that contains fully $\sim$10% of the total molecular material of the Galaxy ($3 - 8 \times 10^7\ M_\odot$ according to the CS measurements: Aharonian et al. (2006), Tsuboi et al. (1999)). The GC GMCs are characterised by supersonic internal velocity dispersions ($\sim 15 - 50$ km s^{-1}: Morris & Serabyn (1996)), high molecular gas kinetic temperature and increased metallicity (Mayer-Hasselwander et al. (1998) and references therein).

The Sgr B complex contains two bright sub-regions, Sgr B1 and Sgr B2, that show up in radio continuum observations (Mehringer et al. 1995; Yusef-Zadeh et al. 2006). The latter is the largest molecular cloud in the Galaxy and contains one its largest complexes of HII regions, being dominated by numerous ultra-compact and hyper-compact H II regions which inhabit three dense cores (labeled North, Main, and South). These are, themselves, located inside a structure labeled the Envelope (Gordon et al. 1993). There have been $\sim$57 UCHII sources identified in Sgr B2(M) alone (Gaume & Claussen (1990), Gaume, et al. (1995) and De Pree, Goss, & Gaume (1998)). The cores are small ($\sim$0.5 pc), light ($10^{3-4}M_\odot$, corresponding to $\sim$5% of the Sgr B2 mass) and dense (10^{6-7} cm^{-3}). On the other hand, the envelope is massive ($7.6 \times 10^5 M_\odot$), and less dense (10^5 cm^{-3}). The average n_{H_2} across Sgr B2 is $\sim 10^6$ cm^{-3}.

Sgr B1, a region of diffuse thermal emission, is comparatively less studied than Sgr B2. It is an HII region of optical depth much less than one at $\sim$ cm wavelengths, suggesting that it is older, evolved structure no longer containing the dense, hot star forming UCHII regions found in Sgr B2 (Mehringer et al. 1995).

2.1. Average Molecular Hydrogen Number Density of Sgr B

In general, for molecular cloud material distributed through the CMZ at a distance $R_{\rm GC}$ from the GC, the minimal number density required in order that the cloud's self-gravity overcome tidal shearing by the central bar potential is given by (Bania et al. 1986; Güsten

1989; Stark et al. 2004; Morris 2007):

$$n_{H_2}^{\rm min} \simeq 10^4 {\rm cm}^{-3} \left(\frac{75 {\rm pc}}{R_{\rm GC}} \right)^{1.8} . \quad (1)$$

The average[2] molecular hydrogen number density over the entire Sgr B complex $\langle n_{H_2} \rangle$ is close to this critical value (given the ~ 100 pc separation between Sgr B and the GC) and lies in the $10^{(3.5-4)}$ cm^{-3} range (Lis & Goldsmith 1989, 1990; Paglione et al. 1998). We adopt a working figure of $\langle n_{H_2} \rangle = 10^4$ cm^{-3} for definiteness.

As may be adjudged from the number densities quoted above, however, one should keep in mind that the distribution of gas across Sgr B is highly clumpy. Nevertheless, we have tested our models of synchrotron emission for injection into such a clumpy medium (as parameterized on the basis of the results set out in Figure 6 of Paglione et al. (1998)) and find that integrated results are in agreement to within 20% (small on the scale of other uncertainties) with those obtained using a one-zone model – as henceforth employed – with average values for molecular density (and magnetic field).

2.2. Average Magnetic Field of Sgr B

The determination of magnetic field strengths through the GC region has been of long-standing interest; a very recent – though not entirely disinterested review – is that by Morris (2007).

The magnetic phenomenology of the GC is dominated by the so-called non-thermal filaments (NTFs; Yusef-Zadeh & Morris (1987); Morris & Serabyn (1996)). The NTFs are remarkable structures: they are magnetic flux tubes of up to 30 pc length but only fractions of pc wide, running predominantly perpendicular to the Galactic plane, and illuminated by synchrotron emission. They are found at distances of up to 150 pc from the GC – across a swathe of Galactic longitude, then, apparently conincident with the CMZ – but not outside this region. Given the almost invariant curvature of the filaments and their regularity – despite clear interactions with the turbulent GC ISM (Morris 2007) – these structures must be quite rigid, consequently allowing the inference of a very large field strength of $\sim$ mG scale (Yusef-Zadeh & Morris 1987; Morris & Serabyn 1996).

A long-standing and on-going controversy concerns the question of whether the $\sim$mG scale magnetic field strength and structure determined for the NTFs is actually pervasive

[2]Note that this is the average over mass at a given density, not the volumetric average

or not. It is beyond the scope of this paper to consider this issue in any detail. Instead, we shall adopt the approach of considering both the upper and lower scales for global GC magnetic field strength argued for by various researchers in the following, viz., ~ 1 mG and $\sim 10\,\mu$G. The assumed strength of this global field shall be of importance when we come to consider whether a central object (located close to or at Sgr A*) is possible as the source for the populations of relativistic particles we infer to be pervading Sgr B.

In any case, the poloidal field structure traced by the NTFs is observed (via far-IR polarization measurements: see Morris & Serabyn (1996), Novak et al. (2003)) to break down in GC molecular clouds. In fact, the field direction inside GC molecular clouds tends to be drawn out along a direction following the ridge of molecular and thermal radio emission, predominantly *parallel* with the Galactic plane, therefore and at right angles to the NTF fields. Such a configuration might arise naturally from the shearing action of the tidal field at the GC on the orbital motion on the molecular gas, drawing an initially poloidal configuration of field lines fixed in the matter into a toroidal one as an inadvertant consequence of differential gas rotation (in a situation where gravitational forces overcome magnetic ones).

As regards Sgr B in particular, the average magnetic field of the complex, especially the average field magnitude over large scales, is somewhat uncertain. A determination of the line-of-sight magnetic field strength $B_{\rm los}$ in the Sgr B2 region of the cloud has also been made on the basis of Zeeman mapping the H I line in absorption (Crutcher et al. 1996). This is 0.48 mG with a spatial variation of around 50 %. Given the resolution of those observations ($5''$ for Sgr B2), this estimate may apply to the outer envelope of the cloud complex (Crutcher et al. 1996). Further, the figure of ~ 0.5 mG is actually a *lower limit* to the average local field strength as line-of-sight field reversals can only reduce the field strength inferred from Zeeman splitting and not increase it (Novak et al. 1997). Also note that, statistically for a large ensemble of molecular clouds, $B_{\rm los} = 1/2\,|\mathbf{B}|$ (Crutcher et al. 1996).

Sub-millimetre polarimetry has also been used to trace the topology of the Sgr B2 field (Novak et al. 1997; Chuss et al. 2005) and, in concert with the Zeeman measurement mentioned above, determines a lower limit to the large scale Sgr B2 field of 150 μG (to be distinguished from the local, presumably somewhat disordered, field directly measured as being at $\gtrsim 0.5$ mG by the Zeeman technique alone). The field structure of Sgr B is revealed by the most recent measurements to be quite complicated (Chuss et al. 2005). The field of Sgr B2 in particular seems to follow a spiral, suggesting an "extreme example of local forces dominating the field structure" (Chuss et al. 2005).

Finally, using results obtained from an ensemble of 27 separate Zeeman measurements of individual molecular clouds and assuming uniform-density spherical clouds, Crutcher (1999)

has derived the following scaling between magnetic field strength and particle number density:

$$B = 0.1 \left(\frac{n_{H_2}}{10^4 \text{ cm}^{-3}} \right)^{0.47} \quad \text{mG}. \tag{2}$$

The Zeeman observation of Sgr B2 (Crutcher et al. 1996) define one of the data points from which this fit is obtained (with an assumed H_2 number density of $10^{3.4}$ cm^{-3}), but it should be noted that the Sgr B2 data point actually falls furthest from (and considerably above) the fitted scaling relation (see Crutcher (1999), Figure 1). Nevertheless, the relation does capture the approximate $\sqrt{n_{H_2}}$ scaling for magnetic field strength that is predicted by many lines of theory (see Crutcher (1999) and references therein), including ambipolar-diffusion-driven star formation. The scaling relation predicts, in our assumed average $\langle n_{H_2} \rangle = 10^4$ cm^{-3}, a field of 0.1 mG.

2.3. Hydrogen Column Density to and through Sgr B

The hydrogen column density *to* Sgr B is estimated to be $\sim 1{\times}10^{23}$ H cm^{-2} (Murakami et al. 2001; Revnivtsev et al. 2004). The column density *through* the densest part of the cloud, the central 2' radius region of Sgr B2, is estimated to be $\gtrsim 8 \times 10^{23}$ H cm^{-2} (Lis & Goldsmith 1989; Murakami et al. 2001). These two values bound the possible range for the average column density to the emission in the one-zone models investigated in this paper (we actually fit to this parameter: see below).

2.4. Temperature of Gas in Sgr B

There is evidence for a least two separate gas components across the CMZ: a 150-200K component as traced by multi-transition ammonia lines (see Yusef-Zadeh et al. (2006) and references therein) and a cooler and denser component with small volume filling factor. There is also a 70 K dust component across the region.

Like the density structure, the temperature structure of Sgr B is complicated and it is therefore difficult to nominate a 'typical' temperature for the gas in this complex. In general across Sgr B2 there is a strong temperature gradient ranging from about 100K at higher Galactic latititudes and longitudes down to about 40K at lower latititudes and longitudes. The dense cores in Sgr B2 are at higher temperatures, $\sim$ 300 K, due presumably to heating by young stars and the surrounding, lower density envelope may be hotter still (600-700K: Wilson et al. (2006)). Furthermore, Wilson et al. (2006) have detected the (J,J) = (18,18) line of NH_3 in Sgr B2 which indicates a very hot component at 600-700K. Sgr B1 hovers at

around 40-50K but does have some hot spots of gas at temperatures up to 90K (Ott 2007).

Also, as mentioned above, the centimeter radio continuum maps show that Sgr B2 has a significant number (∼60) of compact, ultra compact (UC) and hyper compact (HC) HII regions, indicating extremely hot gas, at temperatures of few times 10^3 K on size scale of 10's to 100's of AU dePree et al. (1998), probably due to massive star formation in the dense cores of Sgr B2 Main and North.

Keeping in mind that, given the clumpiness of the density distribution, much of the total mass within the complex is located in the sub-structures named above, we estimate that the typical temperature for gas in the Sgr B complex lies in the range 150-200K.

3. Radio Observations of Sgr B

As described in detail below, we wish to compare the radio flux predictions we arrive at with radio data we have collected from various sources. For fluxes at 330 and 74 MHz (∼90 cm and ∼400 cm) we make use of archival Very Large Array[3] data that covers the region in question (Brogan et al. 2003). At 843 MHz we make use of unpublished data obtained in the course of the Sydney University Molonglo Sky Survey (Bock et al. 1999)[4]. Finally, we have recently observed the dense cores of Sgr B at 1.384 and 2.368 GHz (13 and 20 cm) with the Australia Telescope Compact Array[5] (Jones et al. 2007). In the future we will perform observations with this array in a short baseline configuration that should allow the detection of the non-thermal flux emanating from a relatively large solid angle we predict on the basis of the present work. For the moment, however, the data we have collected were obtained in a baseline configuration relatively insensitive to such flux and provide, therefore, only a rather weak lower limit to the radio flux from the whole Sgr B complex at these wavelengths. On the other hand, we have used these 13 and 20 cm measurement to probe the cosmic ray populations in a number of sub-structures within Sgr B2: see Jones et al. (2007).

We have obtained 74 and 330 MHz VLA maps (Brogan et al. 2003) of the Sgr B region both obtained with a beam of $\sim 1' \times 2'$. The short baseline coverage with which these maps were obtained implies a sensitivity to diffuse flux from scales of up to 6° at 74 MHz and 1-2°

[3]The Very Large Array (VLA), as part of the National Radio Astronomy Observatory, is operated by Associated Universities, Inc., under cooperative agreement with the National Science Foundation.

[4]The Molonglo Observatory Synthesis Telescope (MOST) is operated by the University of Sydney

[5]The Australia Telescope Compact Array (ATCA) is operated by the Australia Telescope National Facility, CSIRO, as a National Research Facility.

at 330 MHz.

Fluxes at both 74 and 330 MHz were obtained by integrating within the entire $0.5^\circ \times 0.5^\circ$ region defined in Aharonian et al. (2006) and a smaller region of $0.35^\circ \times 0.30^\circ$. Unfortunately for our purposes, 74 MHz emission from the GC region is considerably free-free absorbed by intervening HII regions (Brogan et al. 2003; Kassim 1990) meaning that intrinsic flux is badly determined. Moreover, the Sgr B complex is not obviously detected above background in the map at 74 MHz so the total flux at this frequency over the solid angle of the Sgr B complex only defines a rough upper limit to the flux attributable to the object in question.

The determination of the 330 MHz flux was made by taking the statistics over the region, using the Miriad task *histo*, and multiplying the mean flux within the region by the number of beams within it. The flux derived is 45 Jy with an estimated (RMS) error for the primary beam corrected image of 4 Jy.

Following a similar procedure – but noting the provisos outlined above – the 74 MHz flux from the $0.5^\circ \times 0.5^\circ$ region is 570 $\pm$120 Jy.

We convolved the 330 MHz map to the HESS resolution, using a Gaussian with a standard deviation of $0.07^\circ = 252''$. This is shown as the gray scale of Figure 1. The $0.5^\circ \times 0.5^\circ$ field defined above and from which total radio fluxes were calculated is shown as the larger of the two rectangles and the circle is the smoothed beam size. The peak at 330 MHz region is spatially correlated with the peak of the HESS emission which is given by the contours and sits on top of the Sgr B2 structure. The western lobe of the peanut-shaped radio emission feature sits on top of Sgr B1.

Using the above techniques, we also calculated the total 330 MHz flux from the smaller rectangle displayed in Figure 1 which turns out to be 24 Jansky. The ratio of radio to γ-ray fluxes agrees to better than 20% between the two regions, meaning that the correlation between radio and γ emission is no better (actually slightly worse) for the smaller region when averaged over this scale. We will perform a more sophisticated analysis of the spatial correlation between radio and γ-rays in a future work.

In the map one notes a clear radio signal from the SNR/pulsar wind nebula G0.9+0.1 which does not seem to be correlated at all with γ-ray emission, but one should keep in mind here that this object *has* been detected by HESS as a point source and its flux has been artificially removed from the γ-ray map as discussed below in §4.2.

From unpublished data obtained in the course of the SUMSS data at 843 MHz we have also obtained the total flux from the HESS-defined $0^\circ.5 \times 0^\circ.5$ field covering Sgr B. Because of the strong sidelobes caused by the emission from Sgr A, however, we can only make a

crude flux estimate of 20 ±10 Jy.

The spectral index between the central values of the 330 and 843 MHz fluxes is -0.9, with an allowable range of -0.4 to -1.4 clearly indicating a non-thermal spectrum even granted the large errors on the 843 MHz flux.

4. Other Observations of Sgr B

4.1. X-ray Observations of Sgr B

Galactic center molecular clouds, Sgr B2 in particular, have been intensively observed over the last decade in X-rays. The X-ray data covering Sgr B2 reveal both strong continuum emission and a bright source of fluorescent Fe Kα line radiation within the cloud Sgr B2 that displays an unusually large equivalent width of $\approx$ 2–3 keV.

In our data fitting we use the sub-set of the collection of broad-band X-ray data points assembled by Revnivtsev et al. (2004) (and presented in their Figure 2; we re-display these points in our Figures 3 and 4) that approximately give only the *continuum* emission from Sgr B2. Note that these data points – which are due to ASCA/GIS(Koyama et al. 1996; Murakami et al. 2000), GRANAT/ART-P, and INTEGRAL/IBIS over ascending photon energy – are for observations on somewhat smaller angular scales than the $0.^\circ5 \times 0.^\circ5$ field whose broad-band emission we are trying to model. They do, however, cover a good fraction of the total mass in the Sgr B Complex given the clumpiness of the gas distribution (around $2 \times 10^6\ M_\odot$). In any case, because of the uncertainty introduced by this mismatch we do not try to reproduce the continuum X-ray emission in minute detail in our modeling below. Instead we seek only to broadly match the normalization and spectral index of this emission. Note also that *we do not seek to reproduce the Fe Kα line emission at all in this paper.*

A cloud radiates via X-ray fluorescence when it is illuminated, either internally or externally, by a source of $\sim$ 8 keV X-rays or $\sim$ 30 keV CR ions or electrons. Now, a steady X-ray source embedded within the cloud produces an upper limit to the equivalent width of only $\sim$ 1 keV (see, e.g., Fabian 1977; Vainshtein & Sunyaev 1980; Fromerth, Melia & Leahy 2001). A number of authors have taken the large equivalent width of Sgr B2, then, as evidence for illumination by an external X-ray source located towards the actual GC, usually identified with Sgr A* (see Revnivtsev et al. (2004) and references therein). In this scenario, then, we are witnessing the X-ray echo, delayed by 300–400 years relative to the direct signal from the black hole, due to the light travel time from the Galactic center out to Sgr B2's position (in which time, by hypothesis, the direct source has fallen back into relative quiescence). Fryer et al. (2006) have recently suggested that the large dynamic range (6 orders of

magnitude: Revnivtsev et al. (2004); Fryer et al. (2006)) for Sgr A* required in this scenario is very difficult to account for theoretically and a more plausible transient X-ray source of the appropriate magnitude and in the appropriate direction from Sgr B2 may have been provided by the collision of the expanding shell of the Sgr A East supernova remnant and the so-called 50 km s^{-1} molecular cloud.

An alternative explanation to the hypothesised external X-ray illuminator has been advanced by Valinia et al. (2000); Yusef-Zadeh, Law & Wardle (2002) and Yusef-Zadeh et al. (2006), viz. that non-thermal electrons collide with ambient matter to produce inner-shell ionizations of iron atoms, leading to 6.4 keV line emission, and simultaneously generate bremsstrahlung radiation to supply the observed continuum X-ray emission.

Again the large equivalent width of the line emission is important here: the low energy electron interpretation of the Fe Kα emission would require a metallicity significantly higher – a factor of 3-4 – than solar and Revnivtsev et al. (2004) in fact raise this as a difficulty with the model. But it is already known that GC MCs have metallicities 1.5-2 solar, in general. Thus as Yusef-Zadeh et al. (2006) remark, this scenario only requires that the metalicity of Sgr B2 be 1.5-2 that of surrounding clouds which, given the amount of star formation taking place in this object, is perfectly credible.

In any case, because we do not actually attempt to reproduce the Fe Kα line emission from Sgr B2 in this paper, it is beyond the scope of this paper to go further into this controversy (this issue will be addressed in a later work: Crocker et al. (2007)). Rather, following the lead of Yusef-Zadeh et al. (2006), in the modeling we present below, we will attempt only to reproduce (broadly) the continuum X-ray spectrum of Sgr B2 with bremsstrahlung emission from low energy electrons, either primary or secondary. Whether the Fe Kα emission seen is due to an external X-ray illuminator or, as in the model of Yusef-Zadeh et al. (2006), is actually due to low-energy cosmic ray electron collisions, is immaterial for our purposes: the models for non-thermal particle populations we eventually arrive at would seem to work in either situation.

4.2. TeV γ-ray Observations of Sgr B

Observations of the Galactic centre region by the HESS instrument shortly after its inception led to the detection of a point-like source of $\sim$TeV γ-rays at the dynamical centre of the Galaxy (HESS J1745-2290: Aharonian et al. (2004)) and compatible with the position of the supermassive black hole Sagittarius A* or the unusual supernova remnant (SNR) Sgr A East (Crocker et al. 2005). A deeper observation of the region in 2004 revealed a second

source: the SNR/pulsar wind nebula G0.9+0.1 (Aharonian et al. 2005). Most recently, the HESS collaboration has demonstrated that, after subtracting these two point sources from their map of the GC, residual, fainter features are evident, in particular, emission extending along the Galactic plane for roughly 2° (Aharonian et al. 2006). This foreground-subtracted map is displayed as the contours in Figure 1.

The morphology of this diffuse emission correlates well with the distribution of molecular material in clouds as traced by CS emission (Tsuboi et al. 1999) and the spectrum of this emission, which is detected by HESS over more than two orders of magnitude in photon energy, is constant, within systematic errors, across the entire region with a spectral index of ∼2.3. This is appreciably harder than emission detected at ∼ GeV energies across the Galactic plane – the origin of the latter being roughly compatible with creation in collisions of a CRH population of the same shape as that observed locally, viz., a spectral index of ∼2.7. Moreover, the HESS-detected γ-ray emission above 1 TeV is a factor of 3-9 times higher than in the Galactic disk and would seem to require, therefore, a different or additional cosmic ray population in this region.

4.3. GeV γ-ray Observations of Sgr B

In contrast to its clear detection in γ-rays at ∼ TeV energies, Sgr B has not been detected in the 30 MeV - 30 GeV energy range, despite being in the field of view of the EGRET telescope's lengthy observations of the GC region (Mayer-Hasselwander et al. 1998). Indeed, it was explicitly noted by Mayer-Hasselwander et al. (1998) that no localized excess associated with the Sgr B complex was detected by EGRET excluding the possibility of a significantly enhanced CR density in these clouds – *in the appropriate energy range*, of course. The closest source EGRET did detect in these pointings, 3EG J1746-2851, was at first thought to have a localization marginally compatible with Sgr A* or Sgr A East, but was later shown to be perceptibly off-set to Galactic east (Hooper & Dingus 2005; Pohl 2005). This imples that this ∼ GeV source can not be identified with the point source seen by HESS at/near Sgr A* (HESS J1745-2290: Crocker et al. (2005)). The extent of the 3EG J1746-2851 source was closely investigated by Mayer-Hasselwander et al. (1998). They found that, though a point source could not be ruled out, a best fit single source model marginally implied emission (above 1 GeV) such that a flux enclosure angle of radius 0°.6 was required to encompass 68 % of the total flux. This is a solid angle larger than the largest under consideration here (given by the entire Sgr B TeV emission region of $0°.5 \times 0°.5$). Furthermore, the fact that the 3EG J1746-2851 source was only marginally determined to be extended (its HWHM was 0°.7 to be contrasted with the HWHM of the pulsar (GeV)

point sources Vela, Geminga, and Crab at 0°.55) means that at GeV+ energies the Sgr B complex would have been indistinguishable from a point source were it detected by EGRET.

In concert, the non-detection by EGRET of Sgr B and its detection in the same pointings of the source 3EG J1746-2851 imply an upper limit to the γ-ray emission from Sgr B of the same level as the detected flux from 3EG J1746-2851 (though it must be acknowledged here that putative Sgr B flux limits provided by low energy EGRET data points (< 300 MeV) are more indicative than strict because of the growth in the EGRET psf towards lower energies). Moreover, these two, in concert with total molecular mass determinations for Sgr B, further imply that the density of CRHs through Sgr B at $\sim$ GeV-100 GeV energies must not be significantly higher than the local CRH density in the same energy range as noted by Mayer-Hasselwander et al. (1998). This is a significant constraint for our model fitting to obey as explained below.

4.4. Cosmic Ray Ionization Rate in Sgr B2

Recent determinations (van der Tak et al. 2006) of the cosmic ray ionization rate ζ_{CR} in the Sgr B2 Envelope from observations of H_3 O^+ emission lines at 364 and 307 GHz with the Atacama Pathfinder Experiment (APEX) telescope[6] show that ζ_{CR} here is around 4 $\times 10^{-16}$ s^{-1} (with a factor of four uncertainty). The central value is thus an order of magnitude larger than the value determined for local molecular clouds up to a few kpc from the Sun (van der Tak & van Dishoeck 2000) and in the vicinity of the Solar System on the basis of extrapolation of measurements taken by the Pioneer and Voyager spacecraft, viz. 3 $\times 10^{-17}$ s^{-1} (Webber 1998). Van der Tak et al. (2006) have also determined a lower limit for ζ_{CR} in Sgr B2(Main) of around 4 $\times 10^{-17}$ s^{-1} and estimate that the actual value of this quantity is $\sim 1 \times 10^{-16}$ s^{-1} The authors conclude that *the ionization rates of dense molecular clouds are mainly determined by their location in the Galaxy through variations in the ambient CR flux* and that, as a second order effect, ζ_{CR} may be ~ 3 times lower in dense molecular clouds than in diffuse clouds.

In any case, these observations would seem to justify adopting an average ζ_{CR} for the entire Sgr B Complex of 4 $\times 10^{-16}$ s^{-1} – and this may actually be an underestimate.

---

[6]The Atacama Pathfinder Experiment (APEX) telescope is operated by Onsala Space Observatory, Max Planck Institut für Radioastronomie (MPIfR), and European Southern Observatory (ESO).

4.4.1. Cosmic Ray Heating in Sgr B

In passing we note that, employing the results obtained by Suchkov et al. (1993) for the temperature of molecular gas heated by cosmic rays and cooled by molecular line emission (see their Figure 1), the cosmic ray ionization rate given above, together with the assumed average molecular hydrogen number density of 10^4 cm^{-3}, translates into a temperature of $\sim$ 30 K. It seems, then, that given the temperature range also stated above cosmic ray heating cannot be the dominant heating mechanism in Sgr B.

5. Secondary Particle Spectra from CRH Collisions

We wish to model the injection of electrons, positrons and γ-rays into the Sgr B environment through the decay of charged and neutral pions (and heavier mesons) which are themselves created in collisions between hadronic cosmic rays (protons and heavier ions all the way up to Fe) and ambient gas (which is roughly 93% H nuclei – mostly in H_2 molecules in the molecular cloud environment – and 7% He nuclei). To this end, we have employed two Monte Carlo event generators, TARGET 2.1a (Engel et al. 2003) and SIBYLL 2.1 (Engel et al. 2000), that simulate proton-proton collisions at a given energy, to create numerical yield data for secondaries. We employed TARGET, in particular, to generate yields from single p-p collisions between 1.259 and 100 GeV and SIBYLL to generate yields from 100 to 10^6 GeV and these two calculations were smoothed together at 100 GeV. We then used a MATHEMATICA routine to interpolate the yield data for energies intermediate to those directly simulated.

Secondary spectra due to collisions between an arbitrary distribution of beam CR particles with gas in the molecular cloud can be written as

$$q_2(E_2) = \int dE_p \, \frac{dN_p}{dE_p}(E_p) \, n_H \, \epsilon(E_p) \, \sigma_{pH}(E_p) \, \frac{dN_2}{dE_2}(E_p, E_2) \, , \tag{3}$$

where q_2 is in secondaries/eV/s/cm^{-3} with secondary $\in \{e^-, e^+, \gamma\}$;

$$dN_p(E_p)/dE_p = \frac{4\pi \, J_p(E_p)}{\beta(E_p) \, c} \tag{4}$$

is the number density of cosmic ray p's per unit energy pervading the medium; J_p is the differential flux of cosmic rays protons at total energy E_p in cm^{-2} s^{-1} eV^{-1} sr^{-1}; n_H is the number density of H nucleus targets in the gas; $\epsilon(E_p)$ is the (unitless) energy-dependent modification factor introduced by Mori (1997) to account for the presence of heavier ions in

both target and beam[7]; $\sigma_{pH}(E_p)$ is the total, inelastic cross-section for collisions between a beam proton at energy E_2 and a stationary target H nucleus (in cm^2 and as parameterized by Block et al. (2000); and $dN_2(E_p, E_2)/dE_2$ in units eV^{-1} is the (differential) yield function obtained from the interpolation of the Monte Carlos, i.e., the distribution of secondaries with respect to secondary particle energy per interaction of a primary cosmic ray p having energy E_p.

By way of reference, we have calculated the mean energy of the parent beam proton of a γ-ray observed with energy E_γ in a power-law distribution of given spectral index. We tabulate the results of this calculation in an appendix. Similar tables are provided for secondary electrons and positrons.

5.1. 'Knock-on' Electron Production

At low energies – significantly below 10^8 eV – one must account for the fact that the primary source of secondary leptons is no longer from meson decay but rather from thermal electrons directly 'knocked-on' by Coulombic collisions of primary protons and heavier CR ions. In calculating spectra of such electrons we use the results set out in Dogiel & Sharov (1990).

5.2. Relating γ-ray and Secondary Electron/Positron Production

With the above technology we can find, for a given input CRH spectrum, the resulting emissivity of secondary particles. In fact, we can tie together the emissivity of γ-rays and secondary leptons (due to both particle decay and the knock-on process) at a particular energy, given that we know the shape of the initiating CRH spectrum. In other words, we may write:

$$q_e(E_e, \text{spectrum}) = R_{e\gamma}(E_e, \text{spectrum})\, q_\gamma(E_e, \text{spectrum}) \tag{5}$$

[7]This factor is determined from the observed terrestrial CRH spectrum and abundances. It is constant with a value of ~ 1.5 from CR proton energies 1 GeV - 100 GeV, climbing slowly thereafter to be ~ 1.85 at 10^5 GeV. This factor may, of course, actually be an underestimate in the case of the GC environment where a higher supernova rate could imply more heavy ions in the CRH spectrum than detected locally and a larger admixture of heavier nuclei in the target gas.

where q_e denotes the emissivity of secondary electrons + positrons and we have implicitly defined

$$R_{e\gamma}(E_e, \text{spectrum}) \equiv \frac{q_e(E_e, \text{spectrum})}{q_\gamma(E_e, \text{spectrum})} \tag{6}$$

in which the notation $q_2(E_e, \text{spectrum})$ indicates that the emissivity of the secondary is, in general, a function of the input spectrum of CRHs. For a given input spectrum shape, we can numerically calculate $R_{e\gamma}(E_e, \text{spectrum})$ using the results from our interpolation of the pp collision Monte Carlos and, in addition, a contribution from the 'knock-on' electrons identified above (note that in the calculation of $R_{e\gamma}$ n_{H_2} factorizes out). So, for instance, this quantity can be calculated for a power-law spectrum of CRHs parameterized by spectral index γ (the overall normalization of the CRH spectrum factorizes out):

$$R_{e\gamma}(E_e, \gamma) = \frac{q_e(E_e, \gamma)}{q_\gamma(E_e, \gamma)} \,. \tag{7}$$

Even more generally, we can relate the emissivity of electrons + positrons at one energy to the γ-ray emissivity at another:

$$q_e(E_e, \text{spectrum}) = R_{e\gamma}(E_e, \text{spectrum})\, R_\gamma(E_e, E_\gamma, \text{spectrum})\, q_\gamma(E_\gamma, \text{spectrum}) \tag{8}$$

where

$$R_\gamma(E_e, E_\gamma, \text{spectrum}) \equiv \frac{q_\gamma(E_e, \text{spectrum})}{q_\gamma(E_\gamma, \text{spectrum})} \,, \tag{9}$$

which, again, we can of course particularize to the useful case of a power law spectrum of input CRHs.

6. Steady-State Primary and Secondary Electron Distributions

For the Sgr B environment, we have $n_H \sim 10^4$ cm^{-3} and average magnetic fields $B \sim 10^{-4}$ Gauss, implying relatively short energy loss times for electrons and positrons: e.g., the loss time $t_{\text{loss}}(E_e)$ for leptons in this environment reaches a *maximum* of $\sim$ 3500 years for energies around 10 GeV (see Figure 2).

Note that in this work we do not consider non-steady-state lepton distributions at significant length. We introduce this restriction basically to avoid opening up the parameter space by too much: non-steady state models – which will necessarily involve fine-tuning given the short loss timescales mentioned above (see §8.3) – will be investigated in detail in a later work (Crocker et al. 2007).

Now, noting that (i) synchrotron radiation by electrons of ν GHz frequency will be generated by electrons of energy $E_e^{\text{corres}} \simeq \text{GeV}\sqrt{(\nu/\text{GHz})\,(10^{-4}\,\text{Gauss}/B)}$ in the expected

magnetic field strength, (ii) the loss time at GeV is $\sim$ 3000 years, and (iii) taking an absolute upper limit on the diffusion co-efficient in the molecular cloud environment to be given by the value appropriate to the Galactic plane, viz. $D(E) \sim 5.2 \times 10^{28}\,(E/3\,\mathrm{GeV})^{0.34}$ cm^{-2} s^{-1} (Ptuskin et al. 2006), an upper limit on the diffusive transport scale is given by $\sqrt{2D(\mathrm{GeV})t_{\mathrm{loss}}(\mathrm{GeV})} \sim 20$ pc, approximately equal to the radius of the Sgr B Complex. This is likely to be a considerable overestimate of the diffusive transport scale given that, in the turbulent magnetic environment of GC molecular clouds, the diffusion coefficient is likely to be considerably suppressed with respect to its value in the Galactic plane. The above means that diffusive transport can be neglected and, therefore, the ambient number density of electrons + positrons, per unit energy, $dn_e(E_e, \vec{r})/dE_e$ (in $e^{\pm}$ cm^{-3} eV^{-1}), at various positions $\vec{r}$ within the molecular cloud complex, can be obtained in steady-state by numerical integration :

$$\frac{dn_e}{dE_e}(E_e, \vec{r}) = \frac{\int_{E_e}^{\infty} q_e(E'_e, \vec{r}) dE'_e}{-dE_e(E_e)/dt} \tag{10}$$

where $q_e(E'_e, \vec{r})$ is the injected emissivity of electrons + positrons that, in general, might be either primary (i.e., directly accelerated *in situ*) or secondary and $dE/dt(E_e)$ is the total rate of energy loss of electrons at energy E_e due to ionization, bremmstrahlung, synchrotron and, possibly, IC emission (because of the energies involved, we neglect positron annihilation, and assume electrons and positrons suffer identical energy losses). Electrons and positrons lose energy by ionization losses in neutral molecular hydrogen at a rate

$$\frac{dE_e}{dt}_{\mathrm{ioniz}} \simeq -\frac{1.5 \times 10^{-8}}{\beta_e} \times \left(\frac{n_{H_2}}{\mathrm{cm}^{-3}}\right) \times \ln\left[\frac{E_e^2\,\beta_e^2\,(\gamma_e - 1)}{2\,E_{exctn}^2}\right] \quad \mathrm{eV/s}\,, \tag{11}$$

where E_{exctn} is the average excitation of the medium (in the molecular cloud environment of interest we set $E_{exctn} = 15$ eV – see Schlickeiser (2002) p. 99). Electrons and positrons lose energy by bremsstrahlung in molecular hydrogen at a rate

$$\frac{dE_e}{dt}_{\mathrm{bremss}} = -1.7 \times 10^{-15} \times \left(\frac{n_{H_2}}{\mathrm{cm}^{-3}}\right) \times \left(\frac{E_e}{\mathrm{eV}}\right) \quad \mathrm{eV/s}\,. \tag{12}$$

The synchrotron energy loss rate is

$$\frac{dE_e}{dt}_{\mathrm{synch}} = -1.0 \times 10^{-3} \times \left(\frac{B_\perp}{1\ \mathrm{Gauss}}\right)^2 \times \left(\gamma_e^2 - 1\right) \quad \mathrm{eV/s}, \tag{13}$$

where $B_\perp$ is the component of magnetic field perpendicular to the electron's direction. For an isotropic electron population $\langle B_\perp \rangle = 0.78B$.

6.1. Cooled Primary Distribution

In the case that q_e is attributable to a steady-state injection of *primary* electrons, we have no independent, empirical handle on this *injected* population – we only see emission from the *cooled* distribution of electrons. This is to be contrasted with the situation for secondary leptons where high-energy γ-ray emission from neutral meson decay can always provide, in principle, such a handle as explained above.

The cooled electron distribution is steepened at high energies by synchrotron radiation and flattened at low energies by ionization losses. However, for an intermediate range of energies around $\sim$ GeV (depending on the exact details of the magnetic field and ambient gas density) – roughly the same energy range as electrons that are synchrotron radiating at $\sim$ GHz wavelengths – bremsstrahlung emission is the dominant cooling process and, because the bremsstrahlung cooling rate has a linear dependence on electron energy, it does not modify an injection spectrum. In particular, cooling of a power-law distribution of electrons injected with a spectral index γ will not modify this spectral index around the $\sim$ GeV scale in a typical molecular cloud environment. These two facts, together with the relation between spectral index of the synchrotron-radiating electron (power-law) distribution and the spectral index of the generated radio spectrum given below in Eq.(14), imply that spectral index measurements between radio fluxes taken in $\sim$ GHz range may give a handle on the *injected* electron distribution spectral index. Furthermore, once this fixed normalization point has been obtained, provided the magnetic and gas environment of the region in which the synchrotron emitting electrons is located is known, the spectral distortions introduced by ionization and synchrotron, at low and high energies respectively, may be calculated so that the overall shape of the cooled electron spectrum may be determined. Finally, the overall normalization of the cooled distribution may also be obtained given that the distance to the emitting region is known. Putting all these together – as we do in a numerical routine – and assuming *a priori* that the injection spectrum for primary electrons should be a power-law in momentum (as described above) allows one to obtain the injection spectrum: this is simply the power-law distribution characterised by an overall normalization and spectral index that, once cooled by the ionization, bremsstrahlung, and synchrotron processes in the known n_{H_2} and magnetic field reproduces the observed radio spectral index and overall flux.

7. Radiative Processes of Interest

7.1. Synchrotron Emission

The synchrotron emission coefficient (for both primary and secondary electrons) can be calculated using standard formulae in synchrotron radiation theory (Rybicki & Lightman 1979)

$$\begin{aligned} j_\nu(\nu,\vec{r}) &= 1.87\times10^{-30}\,\frac{\mathrm{Watt}}{\mathrm{Hz\,sr\,cm^3}}\times\left(\frac{B_\perp}{1\ \mathrm{gauss}}\right)\int_{m_ec^2}^{\infty}F(\nu/\nu_c)\,\frac{dn_e(E_e,\vec{r})/dE_e}{\mathrm{cm^{-3}}}\,dE\ , \\ \nu_c &= 4.19\times10^6\times(E/m_ec^2)^2\times(B_\perp/\ 1\ \mathrm{gauss})\ \mathrm{Hz}, \\ F(x) &= x\int_x^\infty K_{\frac{5}{3}}(\xi)d\xi, \end{aligned}$$

where $K_{\frac{5}{3}}(x)$ is the modified Bessel function of order 5/3.

Note that, to a good approximation, for a synchrotron-radiating, power-law distribution of electrons with spectral index α, the observed radio spectrum will also be governed by a power law of index α where

$$\alpha=\frac{\gamma-1}{2}\,. \tag{14}$$

7.2. Bremsstrahlung and Inverse Compton Emission

The differential power density originating from bremsstrahlung collisions of $e^\pm$ pervading a medium with atomic number Z and number density n_Z can be determined to be

$$\frac{dP_\gamma^{\mathrm{brems}}}{dE_\gamma}(E_\gamma,\vec{r})=1.7\times10^{-15}\frac{\mathrm{eV}}{\mathrm{s\,cm^3\,eV}}\times\int_{m_ec^2+E_\gamma}^{\infty}\frac{dn_e(E_e,\vec{r})/dE_e}{\mathrm{cm^{-3}}}\,dE_e\,. \tag{15}$$

Similarly, IC emission by a population of electrons $dN_e(E_e)/dE_e$ off a target, thermal photon field characterised by temperature T is approximately given by

$$\frac{dP_\gamma^{\mathrm{IC}}}{dE_\gamma}(E_\gamma)\simeq1.36\times10^{-5}\,\mathrm{s^{-1}}\times\left(\frac{T}{\mathrm{K}}\right)^{5/2}\times\left(\frac{E_\gamma}{\mathrm{eV}}\right)^{-1/2}\times\frac{dN_e}{dE_e}\left(E_e=3.35\times10^7\,\mathrm{eV}\,\sqrt{E_\gamma/\mathrm{eV}\times\mathrm{K}/T}\right)\ , \tag{16}$$

where the Thomson regime is assumed requiring $\sqrt{E_\gamma/\mathrm{eV}\times T/\mathrm{K}}<m_e/\sqrt{2.7\,k_B\,\mathrm{K\,eV}}\simeq3.35\times10^7$. For the Sgr B photon background we assume – to generate an upper limit – energy densities in ultra-violet and dust-reprocessed infra-red light fields the same as that determined for Sgr A East SNR at much smaller Galactic radii ($\sim$ 10 pc), viz., both 5.7 eV

cm^{-3} (Melia et al. 1998). The temperatures of these distributions are taken to be at 30 000 and 20 K respectively. Despite this over-generous attribution of energy into these light fields we find that IC cooling and emission are always sub-dominant to other cooling and radiative processes across the entire lepton spectrum (see below).

7.3. Relating Synchrotron, Bremsstrahlung, and Inverse Compton Emission to γ-ray Emission

With the technology outlined above we can predict on the basis of an observed flux of γ-rays from a particular astrophysical object or region – which must, by hypothesis, orgininate in hadronic interactions of a primary CRH population (i.e, mostly from neutral pion decay) – the radio flux from the same object/region due to secondary leptons. Apart from the γ-ray flux, the inputs to the synchrotron prediction are (i) the $\mathbf{B}$ field strength in the object/region, (ii) the number density of target particles, in our case, molecular hydrogen, n_{H_2}, and (iii) the shape of the cosmic ray spectrum between (a) the energies of CRHs which are responsible for the observed γ-rays and (b) the energies of CRHs which are responsible for the secondary $e^{\pm}$'s whose synchrotron emission we might detect in the radio in some given frequency range.

Significantly, because the synchrotron expectation is normalized directly to the γ-rays, a determination of either the total mass of target particles or the distance to the object/region containing the targets is not necessary in this calculation.

We can use very similar considerations as above to determine predictions for bremsstrahlung emission by secondary leptons. Likewise, with the additional input of the target photon field (radio, IR, optical, UV) we can predict the IC emission by this population of secondaries.

Putting all this together, we can assemble the predicted broad-band spectrum of a particular astrophysical object or region. The calculation is only self-consistent, of course, if, at the γ-ray energy where we normalize our predictions, the γ-rays do strictly originate only in CRH collisions, though a small level of 'pollution' due to IC or bremsstrahlung at the $\lesssim 20\%$ level is perfectly acceptable given other uncertainties.

8. Predicted Sgr B Phenomenology in Hadronic Scenario

8.1. Predicted Sgr B Broad-band Spectrum in Hadronic Scenario

As explained above, adopting the expected, average values $\mathbf{B} = 10^{-4}$ Gauss and $n_{H_2} = 10^4$ cm^{-3} and assuming a power law in momentum for the parent CRH population that,

by hypothesis, is responsible for initiating the $\sim$ TeV γ-ray emission (with spectral index $\simeq 2.3$ and a normalization consistent with this emission), we may determine the broadband spectrum of Sgr B due to all pertinent electromagnetic emission mechanisms (initiated by primary CRHs and secondary leptons). This spectrum is displayed in Figure 3. Here one can see immediately that the model fails to explain any data apart from the gamma-ray flux – though it is not, of course, excluded by the other data. Of particular note, secondary synchrotron does not account for the radio flux detected at 330 MHz (radio datum second from left) or 843 MHz.

One might seek to 'dial-up' the magnetic field strength in the model in order to account for the radio data, but in this endeavor two problems are encountered: (i) the spectral index of the predicted spectrum is rather too flat to go through both 330 and 843 MHz data points (the spectral index between predicted central flux values is -0.31, cf. the observational value of -(0.9 $\pm$ 0.5)) , even allowing for 1-σ excursions of both experimental values and, more tellingly, the magnetic field strength demanded is unreasonably high at 10 mG (as supposed average over the entire Sgr B Complex), implying a magnetic field energy density of 2.6×10^6 eV/cm^{-3}.

8.2. Cosmic Ray Ionization Rate in Hadronic Scenario

Even if we do not rule out such a field *a priori*, there is another reason to reject this model: the contribution of the primary CRH population inferred from the γ-rays is far too small to account for the observed cosmic ray ioniztion rate ζ_{CR} in Sgr B2, viz., 4 $\times 10^{-16}$ s^{-1} as given above. And as stated already, this value should roughly apply over much of the Sgr B Complex.

We may calculate the predicted CRH ionization rate for Sgr B using the technology set out in Webber (1998). Employing the Bethe cross-section

$$\sigma_{\rm Bethe}(\beta, Z) = 1.23 \times 10^{-20} {\rm cm}^2 \frac{Z^2}{\beta^2} \left[6.2 + \ln\left(\frac{\beta^2}{1-\beta^2} \right) - 0.43\,\beta^2 \right] \tag{17}$$

the ionization rate is

$$\zeta_{CR}(J_p, m_{CR}) = \frac{5}{3} \int_{T_p^{\rm min}}^{\infty} 4\pi\, J_p(T_p)\, \sigma_{\rm Bethe}\, dT_p\,, \tag{18}$$

where J_p is the differential flux of cosmic rays protons at kinetic energy T_p in cm^{-2} s^{-1} eV^{-1} sr^{-1} and we take $T_p^{\rm min} \equiv 10$ MeV. To account for the effect of heavier ions in the CRH flux, one may introduce a constant multiplicative factor on the RHS of equation (18) which

is 1.89 for the local CR flux (Spitzer & Tomasko 1968) We note in passing that the above can be directly adopted for calculation of ionization by electrons, though in this case the appropriate energy at which to cut-off the ionization rate integral is $T_e^{\rm min} \equiv 3$ MeV (Webber 1998).

Using these results, the predicted ζ_{CR}, is only 6 $\times 10^{-18}$ s^{-1} and, if the entire non-thermal radio flux is accounted for by secondaries generated by this CRH population, there is no room left for another low-energy particle population whose collisions might account for the ζ_{CR} measurement. Even allowing for a possible additional contribution from heavier ions in the GC environment (relative to their contribution in the Solar System environment) could not make up the $\sim$ two order of magnitude deficit with respect to the ζ_{CR} measured by van der Tak et al. (2006) in Sgr B2.

As a further confirmation that the TeV γ-ray and ionization data are irreconcilable within the current CRH model one may turn around the above logic: for a power-law distribution of CRHs with a normalization sufficient to account for the observed ζ_{CR} one may determine what $\sim$TeV γ-ray spectrum is implied. Carrying out this exercise one finds that the γ-ray flux from Sgr B is overpredicted by around two orders of magnitude.

Of course, it is to be admitted here that to posit a meaningful relation between the ultra-relativistic cosmic rays that generate the TeV γ-rays and the sub-relativistic particle population primarily responsible for ionizing the ambient gas might be considered speculative. Nevertheless, the result stands that these two phenomenological inputs are irreconcilable with the simplest expectation from shock acceleration theory, viz., that the ambient CRHs be governed by a single power law in momentum.

8.3. Double Power-Law Hadronic Scenario

One simple and reasonable modification of the above scenario is to allow for two power-law CRH populations: a steep population, dominant at low energy and with a normalization given by the requirement that it reproduce the observed ionization rate and with a spectral index as flat as possible given the EGRET constraint (implying a value of at least 2.7) and a flatter population of spectral index of $\sim$ 2.2 that becomes dominant at high energy and explains the TeV γ-ray emission. Note that in the GC region it is not at all unreasonable that such a complicated overall spectrum might pertain: the region posseses two and possibly three sources of cosmic rays – unlike other regions in the Galaxy there is activity here associated with the super massive black hole, there is a very high supernova rate and the GC molecular clouds represent a huge reservoir of energy in their turbulent motions.

In any case, we have investigated a double power law scenario and indeed find that for a rather strong average magnetic field, viz., 2.2-3.7 mG (the range implied by the range for the possible total mass of Sgr B Complex), the broadband non-thermal phenomenology is well reproduced. The required energy density in this assumed population is ~ 2.3 eV cm^{-3}, very similar to the local CR energy density (Webber 1998) and, interestingly, the spectral index of this inferred population is very similar to the local one (though one should note that the inferred spectrum, $\propto p^{-2.7}$, is substantially in excess of the local CRH spectrum at 10-100 MeV, explaining how it is possible the former can produce ten times the ionization rate of the local spectrum, despite possessing approximately the same total energy). We have also checked the steady-state positron production rate in this scenario and find that the scenario predicts a 511 keV γ-ray production rate from electron-positron annihilation of $\sim 3 \times 10^{46}$ yr $^{-1}$, well inside the limit by INTEGRAL observations ($\sim 10^{50}$ yr $^{-1}$ out to an angular radius of 8°: Knödlseder et al. (2003); Jean et al. (2003)). The question of the naturalness of this scenario is addressed in the Discussion section but one should note immediately that the energy density in the required magnetic field is 400-1600 times larger than that in the "expected" field given by the Crutcher scaling. In a future publication (Crocker et al. 2007) we will also investigate an inflected primary CRH spectrum – asymptoting to flat power laws at high and low energies but rather steeper at energies in the GeV - 100 GeV range – that holds out the promise of reproducing the broadband phenomenology but for a rather smaller magnetic field.

8.4. Non Steady State Scenario

As stated, we have assumed a steady-state secondary lepton distribution in our calculations above requiring implicitly that the age of the injected lepton distribution is greater than the cooling timescale. If this condition is not satisfied, then, in place of Eq.(10) one has, to tolerable accuracy (Fatuzzo & Melia 2005), that the secondary distribution is given by (injection spectrum) $\times$ (age of lepton population). Now, in consultation with Figure 2, one also notes that the loss time is a strong function of energy with different loss processes dominant at different enegry scales. In fact, one can see from this Figure that it would be possible to fine-tune the assumed age of the lepton distribution in such a way that the leptons predominantly responsible for the observed radio emission (i.e., those at $\sim$ GeV) be out-of-equilibrium, whereas those at lower and higher energies would be in steady state. Now, although the absolute emissivity of the lepton distribution reaches its greatest value when steady state is reached, the greatest emissivity of GeV-scale leptons *relative* to the $\gtrsim$ TeV energy γ-ray emission would be achieved in such a fine-tuned situation (that would require a lepton population of age < 3000 years). Thus, a larger $\sim$ GHz radio emission

could be achived for the same observed $\sim$ TeV γ-ray emission in this somewhat fine-tuned scenario relative to a completely steady state model assumed above. This scenario will be investigated at greater length in a forthcoming publication (Crocker et al. 2007).

9. Predicted Sgr B Phenomenology in Leptonic Scenario

The above considerations naturally lead one to consider the possibility that primary electrons, presumably accelerated in-situ given the short loss times they experience in this strong magnetic field and dense environment, can be invoked to explain the Sgr B phenomenology under consideration.

9.1. The Model of Yusef-Zadeh et al.

Recently Yusef-Zadeh et al. (2006), motivated by their observation of a three-way correlation between the distribution of molecular material across the GC region, Fe Kα line emission, and TeV emission, have considered a model in which a power-law population of primary electrons is invoked to explain the keV to TeV emission from a number of dense molecular regions in the vicinity of the GC including Sgr B1 and B2 inside the Sgr B Complex.

Broadly, these authors' procedure is to determine the local energy density in non-thermal electrons required in order that these particles produce, via their Fe K-shell ionizing collisions, the observed flux of Fe Kα (6.4 keV) X-ray photons. The authors then set the local magnetic field strength to be in equipartition with the energy density in this population and determine the synchrotron emission by the electrons in this field. The magnetic fields arrived at in this way for Sgr B1 and B2 are at the $\sim$ few $\times 10^{-5}$ G level. Yusef-Zadeh et al. (2006) then determine the inverse Compton (IC) spectrum of photons up-scattered from mm wavelengths to TeV+ energies by the inferred high energy component of the same electron population. This mechanism requires electrons with energies in excess of 30 TeV as remarked by Yusef-Zadeh et al. (2006) themselves – a severe challenge given that cooling (dominated by synchrotron emission) is so efficient at these energies with a loss timescale at 30 TeV of only a few decades (for the expected magnetic field strengths given below).

We have repeated the analysis of Yusef-Zadeh et al. (2006) to confirm their findings. Our detailed re-examination reveals, however, that their models for Sgr B1 and Sgr B2 encounter a number of difficulties. Not the least of these is that, in the case of Sgr B2 at least, the model requires an average magnetic field strength that is 0.045 mG, on the order

of one order of magnitude less than actually measured – and set as a *lower limit* – for this object by Crutcher et al. (1996) (and also much less than the B field inferred on the basis of the Crutcher scaling, Eq.(2)).

Another problem for the Sgr B2 model of Yusef-Zadeh et al. (2006) is that, in the average molecular hydrogen density assumed by them, 10^4 cm^{-3}, their assumed power-law, primary electron distribution seems to produce too much bremsstrahlung emission at both $\sim$ 100 MeV and $\sim$ TeV energies, surpassing the EGRET upper limit and also the HESS data points (Yusef-Zadeh et al. actually invoked IC to explain the $\sim$ TeV data, but bremsstrahlung will make an unavoidable – and actually dominant – contribution in this same energy range given that $\sim$30 TeV+ electrons are necessary in order that the IC mechanism work). This objection might be dealt with, however, by invoking a somewhat reduced $n_{H_2} \simeq 5 \times 10^3$ cm^{-3}.

Yet another problem, though, is in what seems to be a lack of self-consistency in the way these authors deal with the cooling of the injected, primary electrons. In their calculation of the energy density in their fitted, equipartition electron population, Yusef-Zadeh et al. assume a pure power-law in electron *kinetic* energy between 10 keV and 1 GeV. Leaving aside the potential issue that the assumption of a power law in kinetic energy (rather than momentum) is a rather unnatural one, the problem here is that ionization loses at low energy should significantly distort an injected spectrum away from such power-law behavior (unless the time from injection of the particles is significantly less than the ionization cooling timescale, $\ll$ 100 yr). Indeed, cooling of the distribution assumed by Yusef-Zadeh et al. (2006) would seem to be necessary in order that bremsstrahlung emission by lower emergy electrons not overproduce continuum X-rays – but then the general procedure of these authors would seem to lack self-consistency as, on the one hand, the X-ray emission is apparently calculated with the cooled distribution but the total energy density in the distribution is calculated with an uncooled (i.e., pure power law) distribution.

9.2. A New Leptonic Model for Sgr B

Because of these difficulties, and to further explore the parameter space, we therefore relax the constraint imposed by Yusef-Zadeh et al. (2006) that the energy density in the electron population be the same as in the magnetic field. We arrive at a satisfactory, alternative lepton scenario to that proposed by these authors in the following fashion: adopting the expected values $n_{H_2} = 10^4$ cm^{-3}, $B = 10^{-4}$ Gauss and $N_{H_2} = 8 \times 10^{23}$ cm^{-2}, we find the *cooled* electron distribution (as parameterized by injection spectral index and normalization) that reproduces the required ζ_{CR} and roughly reproduces the continuum X-ray spectrum of

Sgr B (via bremsstrahlung). We find the spectral index at injection mustbe close to $\gamma = 2.85$.

Fixing γ and also the overall electron population normalization to the values determined by the procedure above, we then determine the B field required in order that the electron spectrum found above reproduce the 330 MHz VLA datum. A very reasonable field of 1.3 10^{-4} G is necessary here for the case of the minimum possible Sgr B mass (the maximum mass case is excluded because it produces significantly too much $\sim$ GeV bremsstrahlung emission contravening the EGRET limit). We subsequently check that the new value of B does not substantially alter ζ_{CR} and the X-ray flux for the already-determined spectral index and normalization.

We then check the $\sim$ GeV bremsstrahlung emission from this distribution (I.C. is subdominant at this energy) in the expected $\langle n_{H_2} \rangle$. Finding that the spectrum now exceeds the EGRET limit, we dial the $\langle n_{H_2} \rangle$ downwards until Sgr B just escapes detection. The required $\langle n_{H_2} \rangle$ is 5×10^3 cm^{-3}. This is very close to the critical number density established by Eq.(1) for molecular gas at a distance of $r_{\rm Sgr\,B} \sim 100pc$ from the actual GC, viz., $\sim 6 \times 10^3$ cm^{-3}.

Again, we determine whether the $\langle n_{H_2} \rangle$ substantially alters ζ_{CR} and the X-ray flux for the previously determined spectral index and normalization. We find that ζ_{CR} is largely unaltered, but the X-ray flux has now decreased. We then vary the final degree of freedom open to us to adjust, the average column density through the cloud and the ISM to the emission region. A satisfactory fit can be determined by dialling this down to be 4×10^{23} cm^{-2} – a value well within the phenomenologically-allowable range.

We have now fully constrained the system and can *predict* the 843 MHz flux. This prediction is 22.3 Jansky, fully consistent with the poorly-determined observational value of 20 $\pm$10 Jy. Given that estimated fluxes might, *a priori*, vary by orders of magnitude, this represents good agreement.

Note that through this procedure we have arrived at an allowable parameter set that is probably not unique and, given the complexities and non-negligible uncertainties surrounding the input data, we have not attempted a χ^2 analysis. Non-trivially, however, we have found a one-zone model for the Sgr B complex that reproduces the broad features of its low-energy, non-thermal phenomenology: a single electron population, injected as a power law in momentum with reasonable spectral index and then cooled by the processes of ionization, bremsstrahlung and synchrotron radiation into a steady state distribution will reproduce the observed cosmic ray ionization rate, the 330 MHz datum and the broad features of the continuum X-ray emission, all for very reasonable values of the ambient magnetic field, molecular hydrogen number density and column density.

We note that the energy density in the cooled electron distribution is 2 eV cm^{-3}. This is

around 10 times the energy density in CR electrons through the Galactic disk as determined by Webber (1998), but considerably sub-equipartition with respect to the energy density in the fitted 1.3 10^{-4} G magnetic field, viz. $\sim$ 400 eV cm^{-3}. Note, however, that the energy density represented by turbulent motions of the Sgr B gas could easily be in equipartition with such a field. In fact, adopting a line width of 10km s^{-1}, as detected for the envelope of Sgr B2 (Lis & Goldsmith 1989), e.g., one determines an equipartition field of $\sim$ 0.7 mG (Novak et al. 1997). One also notes that the inferred energy density is considerably less than that found for the Sgr B1 and B2 regions in the analysis of Yusef-Zadeh et al. (2006), 21 and 51 eV cm^{-3}, respectively. On the other hand it is considerably in excess of the energy density in the broad scale, non-thermal electron population recently inferred by LaRosa et al. (2005). These authors have, on the basis of the application of an argument of equipartition (between magnetic field energy density and relativistic particles) to observations of a large-scale ($6^\circ \times 2^\circ$), diffuse flux of non-thermal radio emission (detected at 74 and 330 MHz) across the GC region, inferred an average magnetic field strength through this region of $\sim$ 15 μG and a non-thermal electron energy density of $\sim$ 0.06 eV cm^{-3} (assuming an electron energy density 1/100 that in protons).

The cooled electron distribution also represents a total energy of 1.1×10^{48} erg. The energy required, however, to have been injected with the un-cooled initial spectrum – and since lost mainly into ionization (thus heating) of the cloud matter – is 1.4×10^{50} erg.

The one respect in which our leptonic model can be said to fail is at TeV energies: it produces far too little bremsstrahlung and IC emission in this energy range to be able to explain the HESS observations. On the other hand it is certainly not in conflict with these observations.

10. A Mixed Model for the Broadband Emission of Sgr B

We are finally, then, led to consider a hybrid model in which a relatively steep population (at injection) of low energy electrons is responsible for the bulk of the measured ionization rate, the 330 and 843 MHz flux and the X-ray continuum flux (via bremsstrahlung), whereas a hard population of CRH's dominates the emission at TeV energies producing the bulk of gamma rays at this energy through neutral pion production and decay. For the broad-band spectrum of such a mixed model, please see Figure 5.

11. Discussion

Both of our models – the double power law CRH model and the mixed lepton/hadron model – require a hard, high-energy (TeV+) spectrum of hadrons to explain the HESS γ-rays. An IC/primary lepton model for this emission – at least as suggested by Yusef-Zadeh et al. (2006) – does not seem to work. As initially noted in Aharonian et al. (2006) and as subsequently explored in Büsching et al. (2006) and Ballantyne et al. (2007), that the spectral index of the diffuse γ-ray emission detected by HESS does not seem to vary over the extent of the CMZ, and, moreover, is so similar to that detected for the central point-like source coincident with Sgr A*, supports the notion that the CRH population responsible for this emission has its origins at relatively small distances from the central black hole and diffuses out into the CMZ from this position. The total energy in this population has been estimated to be 10^{50} erg (Aharonian et al. 2006) marginally consistent with an origin in a single supernova. Furthermore, adopting a diffusion coefficient appropriate to cosmic ray diffusion through the Galactic disk, viz. $D \sim 10^{30}$ cm^2 s^{-1} at several TeV, Aharonian et al. (2006) note that the break-down of the correlation between γ-ray emission and molecular density at angular scales of $\sim 1.3^\circ$ from the actual GC (a position to the East of Sgr B) implies a definite time for the injection event of around 10 000 years, perhaps consistent with the unusual SNR Sgr A East being the source of the CRH population (Crocker et al. 2005).

There are a number of caveats here, however. Firstly, one might expect in such a scenario that – at the periphery of the diffuse emission region (just before the breakdown of the γ-ray/molecular density correlation) – the spectral index of the emission should harden, but such an effect is not seen. Furthermore, the adoption of a diffusion coefficient appropriate to the Galactic disk carries with it a large uncertainty (as noted by Aharonian et al. (2006)). Certainly, if there is a coherent global GC magnetic field of $\sim$ mG strength, then, at the least, the timing of the assumed injection event has to be blow out substantially, and in fact, the whole diffusion-away-from-central-source picture may not be tenable (Morris 2007).

A steady-state picture for the origin of these CRHs – though one still assuming a central source – may be attractive, therefore. One such model that has recently been investigated in the context of stochastic acceleration on the turbulent magnetic field close to the central black hole (Liu et al. 2006) is that of Ballantyne et al. (2007).

11.1. Origin of Putative Steep, Low-Energy Hadron Population

As described at length above, one model that reproduces the broadband phenomenology of the Sgr B Complex consists of a double power law CRH population, the steeper power-law

becoming dominant at low energy. Despite the modest CRH energy density required in this scenario ($\sim$ 2 eV cm^{-3}), one should certainly question the naturalness of such an overall spectrum: if the CRHs are assumed to originate outside the cloud and to be diffusing into it, then exactly the opposite sort of spectral behavior as outlined would be expected, viz., a progressive flattening towards low energies as lower-energy particles find it increasingly difficult to diffuse into the cloud before catastrophic energy loss via hadronic collision on ambient matter in the cloud: see Gabici et al. (2006) and also the companion paper to the current work (Jones et al. 2007).

On the other hand, if the CRHs are accelerated *inside* the GMC, it may be that lower energy CRHs are unable to leave the cloud and naturally accumulate, thereby steepening the overall spectrum towards lower energies, precisely as we require in our model. So, in this scenario, a hard, CRH population – perhaps originating outside the cloud but with sufficient rigidity to penetrate the cloud at high energies – is dominant at HESS energies whereas a population accelerated in situ, and perhaps trapped by the cloud's turbulent magnetic fields, is dominant at lower energies and responsible for most of the Sgr B phenomenology we report.

The total energy in the double power law CRH spectrum is between 1.3-3.3 $\times 10^{48}$ erg, a small fraction of the mechanical energy available from a SN explosion, e.g..

Another question hangs over the magnetic field required in the double power law hadronic scenario. This is, at $\sim$2-4 mG, possessed of an energy density 400-1600 times larger than that of the "expected" field given by the Crutcher scaling as noted above. This scaling relation, however, does not seem to describe the situation in Sgr B2 particularly well, as also already noted. Furthermore, as stressed, the direct Zeeman splitting determination of the Sgr B2 field, at $\sim$ 0.5 mG, actually defines a lower limit to the local average field sgtrength. In fact, both Lis & Goldsmith (1989) and Crutcher et al. (1996) actually countenance average magnetic field strengths as high as $\sim$2 mG for the Sgr B2 cloud on the basis of the theoretical prejudice that the cloud be magnetically supported against gravitational collapse – so we cannot exclude that such field strengths may actually apply on large scales in the complex.

Finally, it must also be admitted that the large magnetic field required may be an artefact of our assumption of a 1-zone model: if p's are accelerated inside the cloud then they will naturally accumulate more in regions where B fields are higher and the synchrotron emissivity resulting from secondaries created by collisions in these regions will also be relatively higher in these locations – so the assumption of an "average" value for the B field may not adequately reflect these effects.

11.2. Origin of Putative Electron Population

In terms of fitting to the broad-band spectrum, the other successful model discovered above is one that invokes a steep ($E^{-2.9}$) primary lepton spectrum at injection together with a hard CRH population to explain the HESS γ-rays.

One notes that the required (steep) electron injection index required in this scenario is well beyond the range normally attributed to shock acceleration, which is typically 2.0-2.4 and, indeed, even a combination of shocks might not allow such an overall steep distribution easily. There do seem, however, to be two plausible instances in which such a steep spectrum might be arrived at: (i) stochastic acceleration off a turbulent magnetic field within the cloud (i.e., acceleration by plasma wave turbulence, a second-order Fermi acceleration process; see, e.g. Petrosian & Liu (2004)), and (ii) shock acceleration with an energy-dependent loss or diffusion. Again, concrete examples of these two general mechanisms will be evaluated in a later work (Crocker et al. 2007).

The energy at injection represented by the putative non-thermal electron population invoked above, 1.4×10^{50} erg, is too big, e.g., to have been supplied by a single, ordinary supernova event (the total energy that goes into non-thermal particles populations and fields being around 5×10^{49} erg; see, e.g. Duric et al. (1995) – but, of non-thermal particles, most energy goes into hadrons).

In this context, however, one notes the possibility that multiple supernovae have occurred within the Sgr B Complex, it being a site of very active star formation and harboring many massive and hot stars. In fact, Koyama et al. (2006a) and Koyama et al. (2006b) have very recently claimed the discovery of a new SNR designated Suzaku J1747.0-2824.5 (G0.61+0.01) on the basis of a detection of an excess of 6.7 keV FeXXV Kα emission from inside the Sgr B region with the X-ray Imaging Spectrometer on board the orbitting *Suzaku* X-ray telescope. Furthermore, on the basis of the CO mapping performed by Oka et al. (1998), Koyama et al. (2006a) and Koyama et al. (2006b) claim the existence of a radio shell in this same region possessed of a kinetic energy of order 10^{52} erg, supporting the possibility of multiple supernovae within the Sgr B Complex.

12. Conclusion

A major result of this work is that we get far too little radio flux from secondary leptons (normalized to the HESS γ-ray data) to explain the VLA and SUMSS observations for reasonable magnetic field values and assuming a power-law (in momentum) behavior of the initiating CRH primaries. Furthermore – making the (perhaps naive) assumption that

the CRHs be governed by a single power law in momentum from ultra-relativistic energies down to the sub-relativistic regime – the cosmic ray ionization rate ζ_{CR} implied by the CRH population inferred from the HESS γ-ray data is far too small to be reconciled with recent determinations of this quantity for Sgr B2. Conversely, a simple interpretation of the ionization rate in this cloud being maintined solely by the CRH distribution would then overproduce TeV photons via pp scattering events compared to what is measured by HESS (again, assuming a pure power law).

Another major result is that it seems almost certain that one needs a hard, high-energy cosmic-ray *hadron* population to explain the HESS TeV+ γ-ray data: a particular model introduced by Yusef-Zadeh et al. (2006) that would seek to explain this emission by inverse Compton scattering by a population of primary cosmic ray electrons seems to break down when considered in detail. Certainly, as for the comsic ray hadron case, a single power-law distribution of primary electrons cannot account for all Sgr B phenomenology.

We have investigated two scenarios that can be reconciled with all the data:

1. A scenario invoking two CRH power law populations (with a steep spectrum dominant at low energy). This scenario requires an ambient magnetic field in the Sgr B Complex in the range 2-4 mG that, while apparently not excluded by existing Zeeman splitting and polarimetry data, may be uncomfortably high. Future submillimetre polarimetry measurements may soon rule in or rule out the necessary field strength. Zeeman splitting measurements at mm wavelengths with the next generation of instruments such as the Atacama Large Millimeter Array (ALMA: Wootten (2006)) may also have sufficient sensitivity to detect these high field strengths, even in lower density regions.

2. Following a path blazed by Yusef-Zadeh et al. (2006), we have investigated the idea that primary electrons play a significant role and, in fact, explain the bulk of the non-thermal Sgr B phenomenology. Unfortunately we find that the particular instantiation of a leptonic model arrived at by Yusef-Zadeh et al. (2006) does not seem to be phenomenologically viable (requiring as it does too small a magnetic field to be reconcilable with the data) or self-consistent (in its treatment of spectral distortion due to ionization cooling at low energies). We have found, however, a leptonic scenario which does satisfactorily account for much of the phenomenology of Sgr B (viz., the CR ionization rate, the X-ray continuum emission, and the 330 and 843 MHz radio emission) but a hadronic component, contrary to the opinions of Yusef-Zadeh et al. (2006), is apparently necessary to explain the gamma-ray emission as mentioned above.

13. Acknowledgements

The authors thank Jim Hinton for providing the HESS data in numerical form and Crystal Brogan for supplying the 74 and 330 MHz data VLA data in numerical form. RMC thanks Roger Clay for discussions about cosmic ray diffusion, Gavin Rowell for advice about the analysis of the γ-ray data, and Troy Porter for advice about the psf of EGRET.

14. Appendix A: Average Parent Proton Energies of Secondaries

Table 1. The average parent CRH energy of a γ-ray observed at E_γ expressed as a multiple of E_γ for various spectral indices.

	2.0	2.2	2.4	2.6	2.8	3.0
10^7 eV	11212.1	3307.03	1492.45	906.29	642.835	494.906
10^8 eV	381.042	93.5398	39.2354	24.2151	18.2917	15.2974
10^9 eV	402.378	124.055	52.8439	29.721	20.0141	15.0221
10^{10} eV	347.006	136.529	64.3183	36.7628	24.5029	18.111
10^{11} eV	196.61	95.9581	49.9323	28.7306	18.4379	13.0247
10^{12} eV	90.378	59.6075	39.3149	26.5121	18.5825	13.6492
10^{13} eV	28.9777	24.4022	20.311	16.792	13.8674	11.5044

Table 2. The average parent CRH energy of a secondary electron observed at E_e expressed as a multiple of E_e for various spectral indices.

	2.0	2.2	2.4	2.6	2.8	3.0
10^7 eV	20509.2	4435.49	1315.68	548.547	305.384	209.977
10^8 eV	839.363	226.115	95.561	56.3558	40.0325	31.4774
10^9 eV	647.868	206.759	88.6688	49.7365	33.3554	24.8667
10^{10} eV	647.707	260.024	117.842	62.529	38.4941	26.6127
10^{11} eV	362.318	194.075	106.836	62.655	39.8574	27.4842
10^{12} eV	143.603	103.072	73.0004	51.8339	37.439	27.8002
10^{13} eV	39.3796	35.013	30.7712	26.7642	23.0849	19.7976

Table 3. The average parent CRH energy of a secondary positron observed at E_e expressed as a multiple of E_e for various spectral indices.

	2.0	2.2	2.4	2.6	2.8	3.0
10^7 eV	4711.5	999.145	368.44	216.004	163.045	138.591
10^8 eV	441.384	114.894	51.1813	32.9168	25.4181	21.4796
10^9 eV	489.759	153.778	66.9793	38.7002	26.6889	20.347
10^{10} eV	525.323	205.124	92.4019	49.6369	31.1947	22.01
10^{11} eV	305.33	160.058	87.2869	51.3001	32.9662	23.0505
10^{12} eV	126.953	89.2382	62.0621	43.4609	31.1185	23.0179
10^{13} eV	36.8475	32.5944	28.563	24.8512	21.5276	18.6259

REFERENCES

Aharonian, F., et al. 2004, A&A, 425, L13

Aharonian, F., et al. 2005, A&A, 432, L25

Aharonian, F. A. et al. 2006, Nature, 439, 695

Ballantyne, D. R., Melia, F, Liu, S., and Crocker, R. M., ApJ *submitted*

Bania, T. M., Stark, A. A., & Heiligman, G. M. 1986, ApJ, 307, 350

Block, M. M. Halzen, F and Stanev. T, 2000, Phys.Rev. D62:077501

Bock, D. C.-J., Large, M. I., & Sadler, E. M. 1999, AJ, 117, 1578

Brogan, C., et al., Astronomische Nachrichten Supplement, 324, 17, 2003.

Büsching, I., de Jager, O. C., & Snyman, J. 2006, ArXiv Astrophysics e-prints, arXiv:astro-ph/0602193

Carson, J. E. 2006, ArXiv Astrophysics e-prints, arXiv:astro-ph/0610960

Chuss, D. T., Dowell, C. D., Hildebrand, R. H., & Novak, G. 2005, ASP Conf. Ser. 343: Astronomical Polarimetry: Current Status and Future Directions, 343, 311

Crocker, R. M., Fatuzzo, M., Jokipii, J. R., Melia, F., & Volkas, R. R. 2005, ApJ, 622, 892

Crocker, R.M., Jones, D., Protheroe, R.J., Ott, J., Ekers, R., and Melia, F. 2007 *forthcoming*

Crutcher, R. M. 1999, ApJ, 520, 706

Crutcher, R. M., Roberts, D. A., Mehringer, D. M., & Troland, T. H. 1996, ApJ, 462, L79

de Pree, C. G.; Goss, W. M.; Gaume, R. A., ApJ, 500, 1998.

Dogiel, V.A., & Sharov, 1990 A&A, 229, 259

Dogiel, V.A., Ichimura, A., Inoue, H., & Masai, K. 1998, PASJ, 50, 567

Duric, N., Gordon, S. M., Goss, W. M., Viallefond, F., & Lacey, C. 1995, ApJ, 445, 173

Engel, R. et al., 2000, Proc. 26th Int. Cosmic Ray Conf. (Salt Lake City, Kieda, D., Salamon, M., and Dingus, B., editors, (AIP, Melville, NY, 2000) volume 1, page 415

Engel, R. et al., 2003, Proc 28th Int. Cosmic Ray Conf. (Tsukuba, Kajita, T., and Teshima, M., editors, Universal Academy Press Inc., Tokyo, Japan) p. 1603.

Fabian, A. 1977, Nature, 269, 672

Fatuzzo, M. and Melia, F. 2005, ApJ 630, 321

Fromerth, M. J., Melia, F., & Leahy, D. A. 2001, ApJ, 547, L129

Fryer, C. L., Rockefeller, G., Hungerford, A., & Melia, F. 2006, ApJ, 638, 786

Gabici, S., Aharonian, F., & Blasi, P. 2006, ArXiv Astrophysics e-prints, arXiv:astro-ph/0610032

Gaume, R.A., Claussen, M.J. ApJ, 103, 1990.

Gaume, R. A., Claussen, M. J., de Pree, C. G., Goss, W. M., Mehringer, D. M., ApJ, 449, 1995.

Gordon, M.A., Bekermann, U., Mezger, P.G., Zylka, R., *et al.*, A&A, 280, 208-220, 1993.

Güsten, R. 1989, IAU Symp. 136: The Center of the Galaxy, 136, 89

Hooper, D., & Dingus, B. 2005, Advances in Space Research, 35, 130

Jean, P., et al. 2003, A&A, 407, L55

Jones, D., Protheroe, R.J., Crocker, R.M., Ott, J., and Ekers, R. *forthcoming*

Kassim, N.E., in *Low Frequency Astrophysics from Space*, N.E. Kassim and K.W. Weiler (eds.), Lecture Notes in Physics (Springer, Berlin), p 144, 1990.

Knödlseder, J., et al. 2003, A&A, 411, L457

Koyama, K., Maeda, Y., Sonobe, T., Takeshima, T., Tanaka, Y., & Yamauchi, S. 1996, PASJ, 48, 249

Koyama, K., Hyodo, Y., & Inui, T. 2006, Journal of Physics Conference Series, 54, 95

Koyama, K., et al. 2006, ArXiv Astrophysics e-prints, arXiv:astro-ph/0609310

LaRosa, T. N., Brogan, C. L., Shore, S. N., Lazio, T. J., Kassim, N. E., & Nord, M. E. 2005, ApJ, 626, L23

Lis, D. C., & Goldsmith, P. F. 1989, ApJ, 337, 704

Lis, D. C., & Goldsmith, P. F. 1989, ApJ, 356, 195

Lis, D. C. & Carlstrom, J. E. 1994, ApJ, 424, 189

Liu, S., Melia, F., Petrosian, V., & Fatuzzo, M. 2006, ApJ, 647, 1099

Mayer-Hasselwander, H. A., et al. 1998, A&A, 335, 161

Mehringer, D., Palmer, P., & Goss, W., 1995, ApJS, 97, 497

Melia, F., Yusef-Zadeh, F., & Fatuzzo, M. 1998, ApJ, 508, 676

Mori, M. 1997, ApJ 478, 225

Morris, M., & Yusef-Zadeh, F. 1989, ApJ, 343, 703

Morris, M., & Serabyn, E. 1996, ARA&A, 34, 645

Morris, M. 2007, ArXiv Astrophysics e-prints, arXiv:astro-ph/0701050

Moskalenko, I. V. and Strong, A. W. 1998, ApJ 493, 694

Murakami, H., Koyama, K., Sakano, M., Tsujimoto, M., & Maeda, Y. 2000, ApJ, 534, 283

Murakami, H., Koyama, K., & Maeda, Y. 2001, ApJ, 558, 687

Novak, G., Dotson, J. L., Dowell, C. D., Goldsmith, P. F., Hildebrand, R. H., Platt, S. R., & Schleuning, D. A. 1997, ApJ, 487, 320

Novak, G., et al. 2003, ApJ, 583, L83

Oka, T., Hasegawa, T., Sato, F., Tsuboi, M., & Miyazaki, A. 1998, ApJS, 118, 455

Ott, J. 2007 forthcoming

Paglione, T. et al. 1998, ApJ 493, 680

Petrosian, V., & Liu, S. 2004, ApJ, 610, 550

Pohl, M. 2005, ApJ, 626, 174

Protheroe, R. 1982 ApJ 254, 391

Ptuskin, V. S., Moskalenko, I. V., Jones, F. C., Strong, A. W., & Zirakashvili, V. N. 2006, ApJ, 642, 902

Revnivtsev, M. G., et al. 2004, A&A, 425, L49

George B. Rybicki, Alan P. Lightman, 1979,"Radiative Processes in Astrophysics" (John Wiley & Sons: New York) .

Rockefeller, G. et al. 2005, ApJ L635, 141

Schlickeiser, R. 2002, Cosmic ray astrophysics / Reinhard Schlickeiser, Astronomy and Astrophysics Library; Physics and Astronomy Online Library. Berlin: Springer. ISBN 3-540-66465-3, 2002, XV + 519 pp.,

Sidoli, L. 1999, Ph.D. thesis, Univ. degli Studi di Milano

Spergel, D. N., & Blitz, L. 1992, Nature, 357, 665

Spitzer & Tomasko, 1968, ApJ, 152, 971,

Stark, A. A., Martin, C. L., Walsh, W. M., Xiao, K., Lane, A. P., & Walker, C. K. 2004, ApJ, 614, L41

Suchkov, A., Allen, R. J., & Heckman, T. M. 1993, ApJ, 413, 542

Sunyaev, R. A., Markevitch, M., & Pavlinsky, M. 1993, ApJ, 407, 606

Sunyaev, R. & Churazov, E. 1998, MNRAS, 297, 1279

Tatischeff, V., Ramaty, R., & Kozlovsky, B. 1998, ApJ, 504, 874

Tsuboi, M., Handa, T., & Ukita, N. 1999, ApJS, 120, 1

van der Tak, F. F. S., & van Dishoeck, E. F. 2000, A&A, 358, L79

Vainshtein, L. A. & Sunyaev, R. A. 1980, Soviet Ast., 6, L353

van der Tak, F. F. S., Belloche, A., Schilke, P., Güsten, R., Philipp, S., Comito, C., Bergman, P., & Nyman, L.-Å. 2006, A&A, 454, L99

Valinia, A., Tatischeff, V., Arnaud, K., Ebisawa, K., & Ramaty, R. 2000, ApJ, 543, 733

Webber, W. R. 1998, ApJ, 506, 329

Wilson, T. L., Henkel, C., Hüttemeister, S. 2006, A&A, 460, 533

Wootten, A. 2006, Astronomical Society of the Pacific Conference Series, 356, 59

Yusef-Zadeh, F., & Morris, M. 1987, AJ, 94, 1178

Yusef-Zadeh, F., Law, C., & Wardle, M. 2002, ApJ, 568, 121L

Yusef-Zadeh, F., Muno, M., Wardle, M., & Lis, D. C. 2006, ApJ (in press), arXiv:astro-ph/0608710

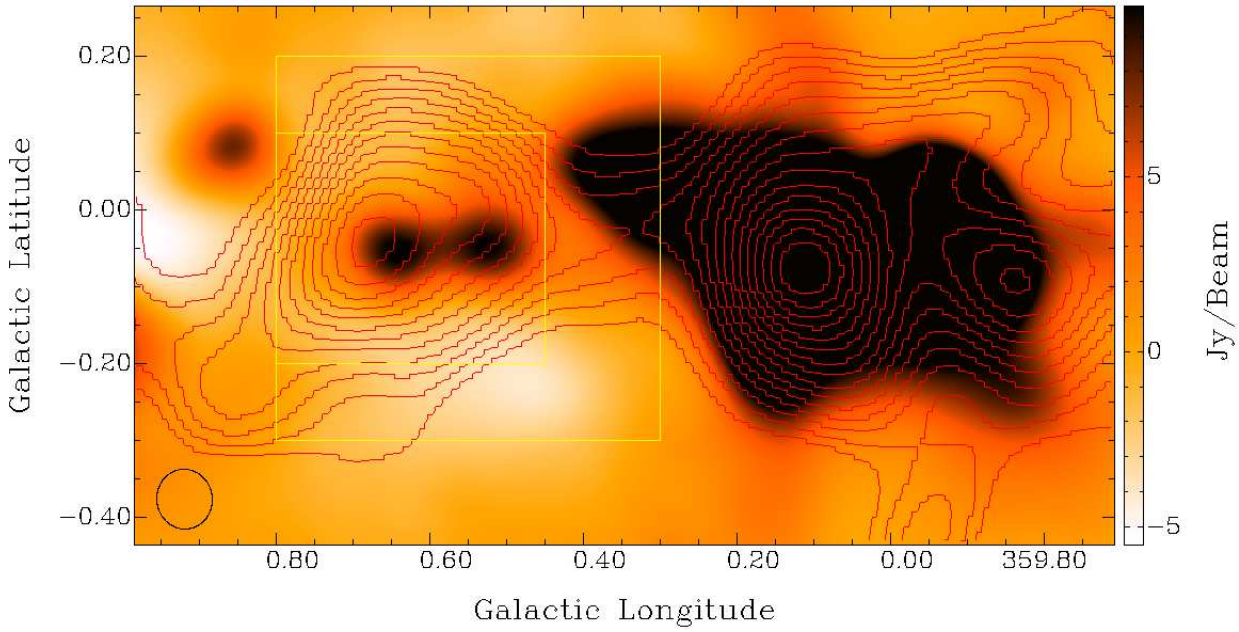

Fig. 1.— Gray scale: 330 MHz VLA data with a position angle of 6° (Brogan et al. 2003) smoothed to match the angular resolution of the HESS instrument (0.07° = 252"; the circle shows the smoothed beam size). Contours: HESS "foreground-subtracted" excess count map for the GC region (Aharonian et al. 2006) with γ-ray flux attributable to the point-like sources coincident with SNR G0.9+0.1 and Sgr A* removed. The contours are from 40% to 90% of total excess counts in increments of 5%. The larger (yellow) box indicates the $0°.5 \times 0°.5$ degree region for which the HESS collaboration provides a γ-ray spectrum. We also calculate the total radio and TeV γ-ray fluxes within the smaller region shown as described in the text. The total radio flux within the smaller box accounts for more than half the total radio flux within the larger box.

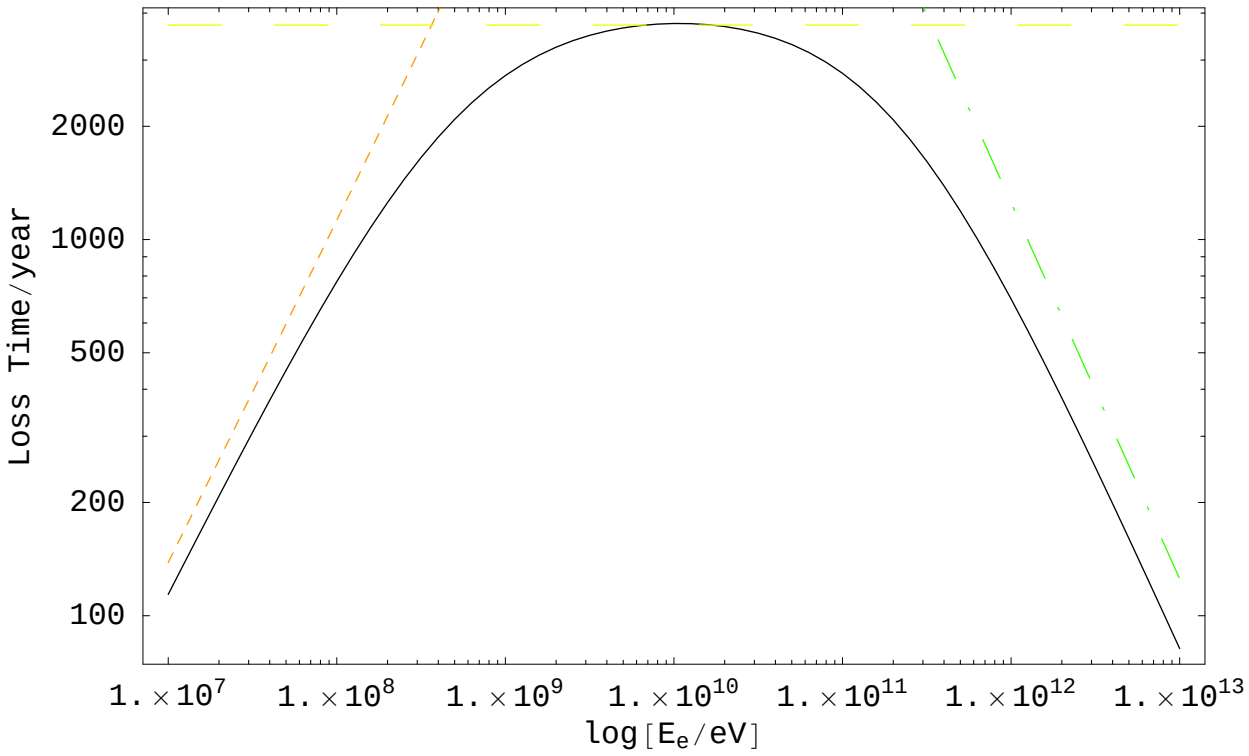

Fig. 2.— Loss times for electrons and positrons in the Sgr B Complex average environment ($n_H = 10^4$ cm^{-3} and $B_{perp} = 10^4$ Gauss). The solid curve shows the total loss time, the small dashed (orange) curve the ionization loss time, the long dashed (yellow) curve the bremsstrahlung loss time, and the long-short (green) dash curve shows the synchrotron loss time. The IC losses are insignificant over this entire energy range and always off the scale of this figure. Note that a steady-state, loss-processed $e^{\pm}$ population requires ∼4000 years to be established in the energy range $1 \gtrsim E/\mathrm{GeV} \gtrsim 100$.

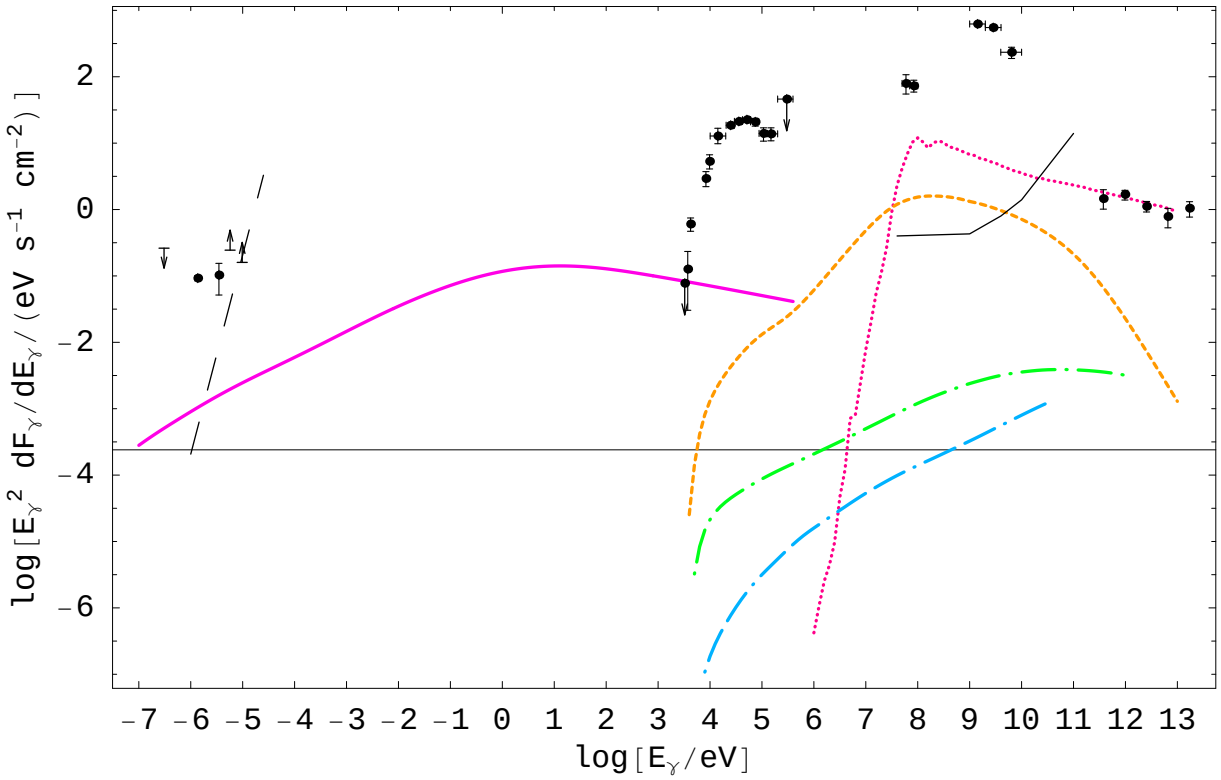

Fig. 3.— The E^2-weighted broadband spectrum of the Sgr B complex as predicted by a π^0-decay model for the TeV emission and assuming a pure power law in momentum for the colliding CRH's with a spectral index of 2.2. A B field of 10^{-4} as determined by the scaling relation of Crutcher (1999), Eq.(2), applied to the average density of the Sgr B Complex, viz. $\langle n_{H_2} \rangle = 10^4$ cm^{-3}. **Data**: radio data points at photon energies $\sim 10^{-(5-6)}$ are obtained from VLA, SUMSS, and ATCA observations. The X-ray data points at $\sim 10^5$ eV are a sub-set of those assembled by Revnivtsev et al. (2004) for the Sgr B2 cloud. The EGRET data points at $\sim 10^8$ eV are a *de facto* upper limit to emission from Sgr B at the indicated energy. The most constraining data points from the spectrum of GC source 3EG J1746-2851 have been selected here. The data points at $\sim 10^{12}$ eV are from the HESS spectrum of Sgr B (the total γ-ray emission from the $0.^\circ5 \times 0.^\circ5$ field indicated by the larger rectangle in fig.(1).) **Fitted emission curves** – dotted (red) line: π^0-decay γ-rays; solid (pink) line: synchrotron emission by secondaries; short dash (yellow) line: bremsstrahlung emission by secondaries; dot-dash (green) line: IC scattered FIR light (20 K, $U_\gamma = 5.7$ eV cm^{-3}); dot-dot-dash (blue) line: IC scattered UV light (30 000 K, $U_\gamma = 5.7$ eV cm^{-3}); long dash (black) line: optically thick thermal bremsstrahlung emission from the UCHII regions contained in Sgr B(Main) and Sgr B(North) with an assumed temperature of 10 000 K and solid angles as given by Gordon et al. (1993). Photo-absorption (at X-ray energies) in the assumed 8×10^{23} cm^{-2} column density is *not* accounted for in calculating the theoretical synchrotron curve. The primary hadrons initiating the secondary leptons that produce the sycnhrotron are assumed to cut off sharply at 10^{16} eV leading to a mirroring cut-off in the synchrotron spectrum at $\sim 4 \times 10^5$ eV. As is immediately apparent, the model fails to explain any data apart from the gamma-ray flux. **Sensitivity curve:** the solid (concave up, black) curve shows $E_\gamma \times$ the projected integral flux sensitivity of the GLAST (Carson 2006) instrument for a 5 σ detection of a point source in 1 year and assuming a $\propto E_\gamma^2$ spectrum: see the GLAST webpage, http://www-glast.stanford.edu.

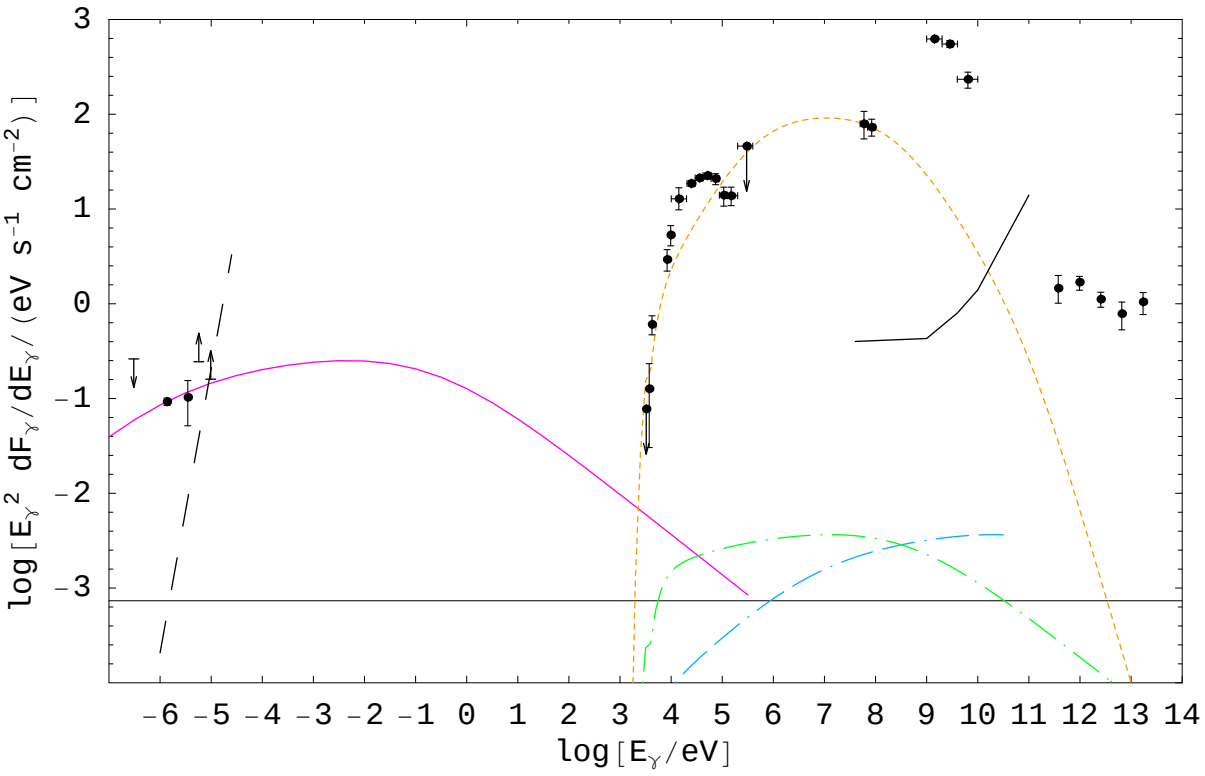

Fig. 4.— The E^2-weighted broadband spectrum of the Sgr B complex as predicted by the primary electron model set out in the text: the primary electron normaliztion and spectral index are determined by fitting to the ionization rate and, broadly, to the X-ray spectrum (we do not seek to reproduce this exactly as described in the text). The B field (=1.3 10^{-4} G) is that required for this spectrum to reproduce the 90 cm datum and the assumed, average molecular hydrogen number density is 5×10^3 cm^{-3} (in order that bremsstrahlung emission obey the EGRET limit). Photo-absorption in the fitted 4×10^{23} cm^{-2} column density is *not* accounted for in calculating the theoretical synchrotron curve. The synchrotron curve is taken to cut off sharply at $\sim 4 \times 10^5$ eV mirroring an assumed cut-off in the primary electron spectrum at $\sim 10^{14}$ eV. Processes corresponding to various curves are as described in fig. 3.

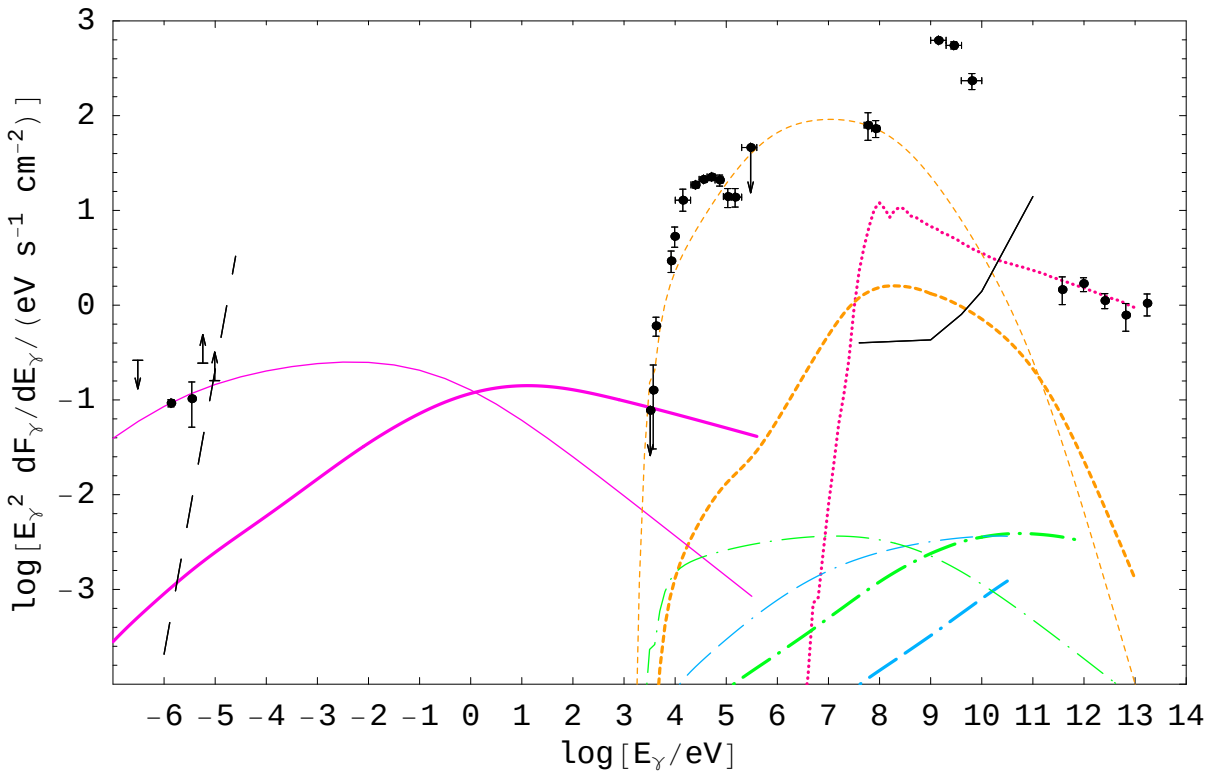

Fig. 5.— A hybrid model for the broadband emission of the Sgr B Complex invoking neutral meson production in CRH collisions and subsequent decay to explain the observed TeV gamma rays and a primary electron distribution to explain the remainder of the pertinent phenomenology. Processes corresponding to various colored curves are as described in fig. 3, thick curves correspond to emission by secondary particles created in hadronic collisions and thin curves to emission by primary leptons (the dashed black curve is thermal bremsstrahlung emission as described in fig.(3)).